Multilayer Ionic Transducers

by

Barbar J. Akle

Thesis submitted to the Faculty of the
Virginia Polytechnic Institute and State University
in partial fulfillment of the requirements for the degree of

Master Of Science

in

Mechanical Engineering

Donald J. Leo, Chair
Daniel Inman
William Saunders

April 2003

Blacksburg, Virginia

Keywords: Ionic Polymer, Multilayer, Sensor-actuator, Micro Air Vehicle.

Multilayer Ionic Transducers

Barbar J. Akle, MS
Virginia Polytechnic Institute and State University, 2003
Advisor: Donald J. Leo

Abstract

A transducer consisting of multiple layers of ionic polymer material is developed for applications in sensing, actuation, and control. The transducer consists of two to four individual layers each approximately 200 microns thick. The transducers are connected in parallel to minimize the electric field requirements for actuation. The tradeoff in deflection and force can be controlled by controlling the mechanical constraint at the interface. Packaging the transducer in an outer coating produces a hard constraint between layers and reduces the deflection with a force that increases linearly with the number of layers. This configuration also increases the bandwidth of the transducer. Removing the outer packaging produces an actuator that maintains the deflection of a single layer but has an increased force output. This is obtained by allowing the layers to slide relative to one another during bending. A Finite Element Analysis (FEA) method capable of modeling the structure of the multilayer transducers is developped. It is used to model the interfacial friction in multilayer transducers.

Experiments on transducers with one to three layers are performed and the results are compared to Newbury's equivalent circuit model, which was modified to accommodate the multilayer polymers. The modification was performed on four different boundary conditions, two electrical the series and the parallel connection, and two mechanical the zero interfacial friction and the zero slip on the interface.

Results demonstrate that the largest obstacle to obtaining good performance is water transport between the individual layers. Water crossover produces a near short circuit electrical condition and produces feedthrough between actuation layers and sensing layers. Electrical feedthrough due to water crossover eliminates the ability to produce a transducer that has combined sensing and actuation properties. Eliminating water crossover through good insulation enables the development of a small (5 mm x 30 mm) transducer that has sensing and actuation bandwidth on the order of 100 Hz.

Due to the mechanical similarities of ionic transducers to biological muscles and their large flapping displacement capabilities we are studying the possibility of their use in flapping Micro Air Vehicle (MAV) application, as engines, controllers and sensors. The FEA modeling technique capable is used to design two ionic polymers actuated flapping wings.

To my father,

Jawad Akle,

my mother,

Nazira Akle,

and my sister and brothers,

Angele, Etienne, and Simon

Acknowledgments

First I would like to thank my advisor, Dr. Donald J. Leo, for his help and patience throughout my graduate studies. His guidance and complete support made my working and learning experience, a very special one. Also, I want to extend my thanks to Dr. Daniel Inman and Dr. William Saunders for their support and enthusiasm as members of my advisory committee.

In addition, I want to thank my colleagues in the Center for Intelligent Material Systems and Structures (CIMSS). The good humor of everybody made it an enjoyable experience. Also my great thanks to my research partners Mathiew Bennet, Kevin Farinholt, John Franklin, and Curt Cothera. Their generous help and friendship was invaluable in assisting my research. I appreciate the support of the U.S. Army Research Laboratory and the U.S. Army Research Office under contract/grant number DAAD19-02-1-0275 Macromolecular Architecture for Performance (MAP) MURI.

Finally, I would like to express my deep gratitude to the support I received from my friends at Emilio's and my greatest appreciation to the love and support provided by my parents and my brothers and sister during my years at Virginia Tech.

Barbar J. Akle

Contents

Abstract ii

Acknowledgments v

List of Tables x

List of Figures xi

Chapter 1 Introduction 1

1.1 Problem Statement 1

1.2 Literature Review 3

1.2.1 Electro-Active Polymers (EAP) 4

1.2.2 Historical Background of Ionic polymers 4

1.2.3 Manufacturing of Ionic polymers 4

1.2.4 Actuation Mechanism 6

1.2.5 Interesting properties of Ionic polymers 8

1.3 Initial Motivation 8

1.3.1 Potential applications 9

1.4 Overview of Thesis 10

1.4.1 Research Objectives 10

1.4.2 Contribution 11

1.4.3 Approach 13

Chapter 2 Experimental Setup 15

2.1 Introduction 15
2.2 Experiments Output 15
2.3 Types of Experiments 16
2.3.1 Electrical Impedance 16
2.3.2 Mechanical Impedance 17
2.3.3 Sensor Sensitivity 19
2.3.4 Blocked Force 19
2.3.5 Free displacement 20
2.4 Equipment Description 21

Chapter 3 Characterization of Ionic Polymer Stacks 24
3.1 Introduction 24
3.2 Stacking techniques 24
3.2.1 Series stacking 25
3.2.2 Parallel stacking 26
3.2.3 Comparison 26
3.3 Sensor Stacks 27
3.3.1 Comparison of Series and Parallel Multilayer Sensors 29
3.3.2 Amplifier Variation 30
3.4 Actuator Stacks 36
3.4.1 Comparing Series and Parallel Stacks as Actuators 36
3.4.2 Interfacial Friction and Mechanical Properties 39
3.5 The Finite Element Analysis method 43
3.5.1 Verification of the FEA method 45
3.5.2 FEA simulations for the parallel stacks 46
3.5.3 Analysis of the interfacial friction 48
3.6 Summary 49

Chapter 4 Combined Sensor-Actuator Stacks 51
4.1 Introduction 51
4.2 Combined Sensor vs. Self-sensing Actuator 51

4.3 Alternative configurations 53
4.4 Fabrication 53
4.4.1 Electrical connections 53
4.4.2 Mechanical properties and the FEA method 56
4.5 Characterization of the combined stacks 56
4.6 Feed-through 59
4.6.1 Insulation 61
4.6.2 Characterization of feed-through 62
4.7 Summary 62

Chapter 5 Modeling multilayer stacks 63
5.1 Introduction 63
5.2 Model Overview 63
5.3 Describing and Modifying the Electromechanical Terms for Multilayer Stacks 65
5.3.1 The Electrical Terms 65
5.3.2 The Mechanical Terms 66
5.3.3 The Electromechanical Term 68
5.4 Modified Input-Output Relationships for Multilayer Transducers. . . 70
5.4.1 Impedances 70
5.4.2 Actuator Equations 71
5.4.3 Sensor Equations 72
5.5 Comparison of Model with Experimental Results 74
5.6 Summary 75

Chapter 6 Micro Air Vehicle 77
6.1 Introduction 77
6.2 Application: MAV 77
6.2.1 Design Parameters 78
6.2.2 Wing Designs 78
6.2.3 Comparison to requirements 79

6.3 Summary 80

Chapter 7 Summary and Conclusions 81

7.1 Introduction 81

7.2 Thesis Summary 81

7.3 Contributions to the Field 83

7.4 Conclusion 84

7.5 Future work 84

Bibliography 87

Vita 89

List of Tables

1.1 Changes on the cathode and the anode of four actuation mechanisms (Bar-Cohen, 2001) 7

4.1 Material property comparison between ionic polymers and piezo PSI-5A4E ceramic (Newbury (2002) and Piezo Systems (2003)) 52

List of Figures

1.1 (a) A schematic drawing showing the hystereses of polymers during operation and (b), the relaxation. 2

1.2 Schematic of an Ionic Polymer. 5

2.1 Schematic drawing showing the experimental setup for the blocked force test. 17

2.2 Schematic drawing showing the experimental setup for the blocked force test. 18

2.3 Schematic drawing showing the experimental setup for the blocked force test. 19

2.4 Schematic drawing showing the experimental setup for the blocked force test. 20

2.5 Fixture 1. 21

2.6 A picture showing the new fixture with details on the parts. 23

3.1 A CAD drawing showing the different parts of a series stack. 25

3.2 Schematic representation of the electric connection for a series stack. . . . 26

3.3 A CAD drawing showing the different parts of a parallel stack. 27

3.4 Fabrication a 3 layers parallel stack. 28

3.5 Schematic representation of the electric connection for a parallel stack. . . 29

3.6 The transfer function of parallel stacks with 1, 2, 3, and 4 layers. 31

3.7 The transfer function of series stacks with 3 and 4 layers plotted with two different single layers polymers. 32

3.8 Transfer function of the same polymer but with a different value of R_1 in the amplifier circuit 33

3.9 Transfer function of the same polymer but with a different value of R_2 in the amplifier circuit 34

3.10 Transfer function of the same polymer but with different amplifier circuits 35
3.11 The Blocked force step response of the differently layered parallel stacks . 37
3.12 The Blocked force transfer function of the differently layered parallel stacks 38
3.13 The blocked force transfer function of series multilayered actuators 39
3.14 A cantilevered beam with an applied pressure w. 40
3.15 Step response for unpackaged parallel stacks 41
3.16 Frequency response function for unpackaged stacks parallel stacks 42
3.17 Step response for packaged parallel stacks 42
3.18 Natural frequency variation of packaged stacks 43
3.19 The free displacement frequency response for packaged stacks 44
3.20 The 2D planar model output for the free displacement step input 45
3.21 The 2D planar model output for the blocked force step input 46
3.22 The 2D planar model output for the blocked force step input 47
3.23 The experimental and FEA outputs for packaged and unpackaged free displacement step output as a function of number of polymers. 48
3.24 The experimental and FEA outputs for packaged and unpackaged blocked force step output as a function of number of polymers. 49

4.1 A 3D CAD drawing representing the combined stack. 54
4.2 Schematic drawing showing the electric connections of the combined stack 55
4.3 Two FRF function for the same stack, one sensed with a polymer sensor and the other with laser vibrometer. 57
4.4 The experimental and model transfer functions of the actuator. 58
4.5 The experimental and model transfer functions of the sensor. 59
4.6 The FRF of different combined stacks, one with feed through and the other without. 60
4.7 Schematic drawing showing the feed through between the sensor and the actuator 61

5.1 The geomertic parameters of the stack. 65
5.2 Electrical impedance model prediction versus experimental data 73

5.3 Sensitivity model prediction versus experimental data 73
5.4 Blocked force model prediction versus experimental data 73
5.5 Mechanical impedance model prediction versus experimental data 74

6.1 The deflection color map output of the FEA analysis of the first wing design. 79

Chapter 1

Introduction

Multilayered stacks of ionic transducers have been developed and characterized in the Center of Intelligent Materials and Smart Structures (CIMSS) Lab at Virginia Tech. They were configured as sensors, actuators, and combined sensor-actuators stacks. They were connected in series, and in parallel. The following chapters are related to the exploration of the stacking process, characterizing it, modeling it, and studying its possible applications.

1.1 Problem Statement

Ionic Polymers are soft transducers which belong to the family of Electro-Active Polymers (EAP). They have several interesting mechanical properties, especially their large displacement, large sensitivity to motion, and low operation voltage. On the other hand, ionic polymers face several disadvantages, especially in the small forces they can generate.

In addition to small force output, ionic polymers exhibit 'permanent strain' effects and relaxation that is detrimental to their use as electromechanical actuators. Figure 1.1 (a) is an illustration of the permanent strain effect. This effect occurs when the polymer is excited with a step voltage and then the electrodes are placed at ground. The resulting motion of the material produces a non-zero permanent strain that is attributed to permanent charge redistribution within the polymer (Newbury,

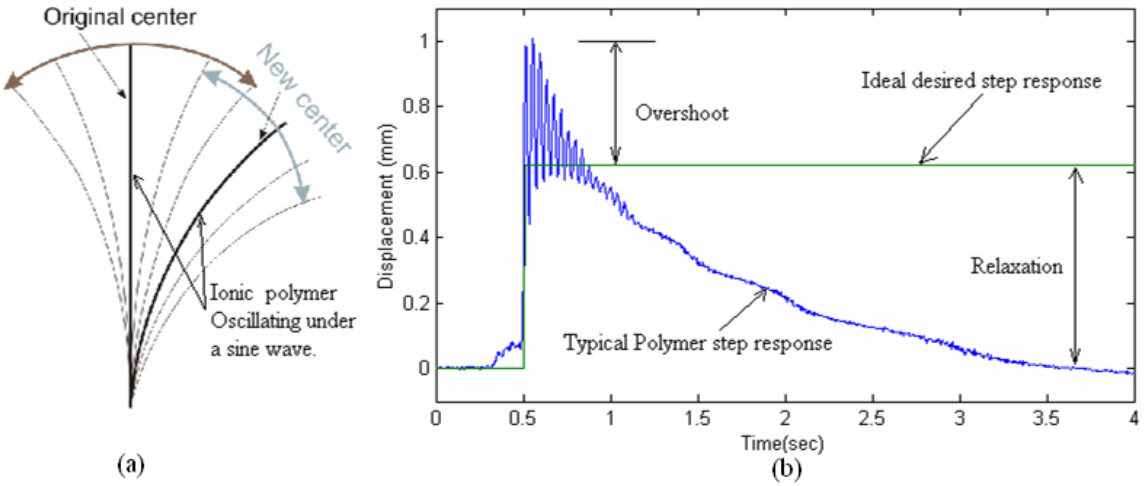

Figure 1.1: (a) A schematic drawing showing the hystereses of polymers during operation and (b), the relaxation.

2002). In addition to permanent strain, several researchers have noted that certain ionic polymer transducers exhibit a relaxation phenomenon when subjected to step changes in the voltage (see Figure 1.1). This relaxation phenomenon reduces the quasi-static actuation authority of the actuator.

Stacking techniques were developed in order to increase the generated force of ionic polymer actuators. Initially we started stacking the single-layer ionic polymers electrically in series, which is simply laying the strips of polymers on top of each other and apply the electric potential across the whole stack. Series stacking solved only part of the problem. It provided higher saturation voltage, but kept the force per overall voltage approximately the same as the single layer polymer. Therefore the series stack did not perform better than the single layer polymer if we comply with the electrolysis start voltage. In order to increase the voltage per layer, and increase the overall generated force without increasing the voltage per stack, we developed parallel stacks. Parallel stacks are single layers ionic polymers overlaid on top of each other mechanically, and connected in parallel electrically. The result is a stack that generates larger forces without exceeding the electrolysis limit voltage. This technique worked properly and encouraged us into further investigations.

Stacking of ionic polymers not only solved the problem of small forces but also proved to resolve the problem of the complex non-uniform behavior. Non-uniformity

in ionic polymers could be defined as hysteresis, relaxation, and the permanent strain previously defined. It has been proven that those non-uniform behaviors could be solved using feedback control (Kothera, 2002). In order to accomplish feedback control, a sensor polymer was inserted inside a stack of several actuators. This sensor polymer was insulated, and connected to a sensing circuit so it fed back the motion. This formed the combined sensor-actuator stack. Results demonstrate that the largest obstacle to obtaining good performance is water transport between the individual layers. Water crossover produces a near short circuit electrical condition and produces feedthrough between actuation layers and sensing layers. Electrical feedthrough due to water crossover eliminates the ability to produce a transducer that has combined sensing and actuation properties. Eliminating water crossover through good insulation enables the development of a small transducer that has sensing and actuation capabilities. Moreover, for design purposes a simulation tool was essential to model all those stacking processes, therefore Finite Element Analysis (FEA) method was used and validated by comparing its output to the experimental results. The FEA method was able to model complex actuator geometries, but the analysis was only valid to the low frequency response. The limitations of the FEA method motivated us to adapt Newbury constuitive model to handle the multilayer stacks. Newbury's model (Newbury, 2002) is capabable of modeling simple cantilever geometry transducers, as sensors and actuators for any type of response. Finally all the tools and results were used to set forth for a design of an Ionic Polymer flapping MAV.

1.2 Literature Review

In this section, a brief background information on Ionic Polymers is provided. The review has started with the definition of the Electro-Active Polymers. Next a chronological historical background is provided and followed by a brief overview on the manufacturing technique and the operation mechanism. Finally, the interesting properties and the potential applications of ionic polymers are explored.

1.2.1 Electro-Active Polymers (EAP)

Electroactive polymers belong to the family of active materials. Active materials are defined as materials that adapt to a change in the physical environment, such as electrical, thermal, magnetic, chemical, pH, or light environment. They can be used in the form of sensors, actuators, active dampers, and energy generators. (Leo course notes, 2001) EAP reacts to the change in the electrical domain, like the widely used and well known electroactive materials such as piezoelectric ceramics. Recent developments in the Electroactive Polymers (EAP) have lead to increasing interest in them, due to there flexibility which makes them similar to biological muscles.(Bar-Cohen et al., 1999) They are also defined in four categories, gels, ionic polymers, conducting polymers, and electrostrictive polymers. In this thesis the interest is in ionic polymers.

1.2.2 Historical Background of Ionic polymers

Polymer-metal composites were developed as early as 1930's as precipitation of colloidal Silver on prepared substrates (Bar-Cohen, 2001). In the early 1990's when Sadeghipour et al. were trying to use ionic polymers as pressure transducers, they found that they could act as vibration sensors. Ionic polymers were developed as "solid polymer electrolyte fuel cell membranes" (Bar-Cohen, 2001). Later in 1992 while Sadeghipour and coworkers were getting close to discover their actuation capabilities, Oguro's group in Japan described the bending of the ionic polymers under the application of a potential across its thickness. Since than, several groups in the USA and across the world are working on improving the manufacturing process, characterizing and modeling the performance, and searching for applications for this new intelligent material.

1.2.3 Manufacturing of Ionic polymers

Presented here is the general method by which ionic polymers are manufactured, although several variations in their manufacturing have been reported (Bar-Cohen,

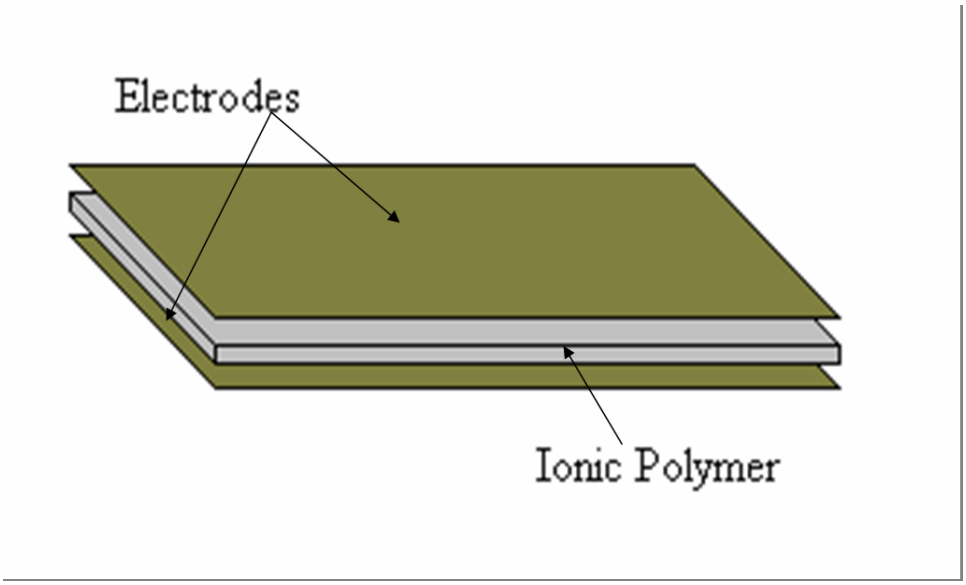

Figure 1.2: Schematic of an Ionic Polymer.

2001). As shown in Figure 1.2 ionic polymers consist of an Ionic polymer membrane sandwiched between two metal overlayers.

The materials used in manufacturing ionic polymers are a strong acid, a metal salt, a reducing chemical solution, and perfluorinated ionomer membrane. Although they are not necessarily the best material to be used in ionic polymers, DuPont's Nafion™ proved to have the best performance in the commercial ionic polymers. The manufacturing process is usually composed of three main steps. After cleaning the polymer with a strong acid such as HNO_3, a clean sheet of polyperfluoroethylene-sulfonate membrane (Nafion™) is soaked in a metal salt solution ($Pt(NH_3)Cl_2$) to populate it with a reducible metal (Bar-Cohen, 2001). During this step the metal salt will exchange hydrogen ion in the polymer backbone. Than this sample is submerged in a chemical reductant such as Lithium Borohydride ($LiBH_4$), which can't penetrate the ionic polymer, thus the reduction will occur according to equations (1.1) and (1.2) only at the surface of the polymer.

$$LiBH_4 + 4[Pt(NH_3)_4]^{2+} + 8OH^- \rightarrow 4Pt^0(s) + 16NH_3(g) + LiBO_2(sd) + 6H_2O \quad (1.1)$$

and

$$LiBH_4 + 4H_2O \rightarrow 4H_2(g) + LiOH\,(Li^+ + OH^-) + B(OH)_{3(sd)} \qquad (1.2)$$

Equation (1.2) provides the hydroxyl ions needed in equation (1.1), therefore 9 moles of LiBH4 are required to reduce 4 moles $[Pt(NH_3)_4]^{2+}$. Notice in equation (1.1) that the products are platinum metals which form the dendritic electrode. The ammonia gas will evaporate and the Lithium Boroxide will precipitate. As for equation (1.2), the hydrogen gas will evaporate the $B(OH)_3$ precipitate, the hydroxyl ion will react according to equation (1.1), while the Lithium ion will chain with the polymer inside the clusters.

Currently several researchers are working on optimizing this process. The surface conductivity is essential in charging the membrane (Bar-Cohen, 2001). In the CIMSS lab, Matt Bennett has been working on this problem, and further trying to incorporate inexpensive metals such as copper into the conducting overlayer. Finally a third manufacturing step might be required to exchange the cation with another one (e.g. replace the Na+ with Li+), which will effect the performance of the ionic polymer as it will be described later.

1.2.4 Actuation Mechanism

To date the physical mechanisms that produce actuation are still uncertain. Several researchers are suggesting different actuation models. The real actuation mechanism could be one of those models, or a combination of them. All of those models consider the polymer's ionic membrane as hydrophilic clusters inside the hydrophobic fluorocarbon polymer backbone.

The main assumption is that anions in the clusters are attached to the fluorocarbon backbone (Bar-Cohen, 2001), while the free cations will move within the water medium under the application of an electric field, causing them to migrate towards the cathode. This redistribution will cause some changes in the properties of the polymer membrane at the anode and cathode sides. Table 1.1 delineate those changes.

Anode	Cathode
Decrease in the effective stiffness of the membrane	Increase in the effective stiffness of the membrane
Generation of a repulsive electrostatic force between the fixed anions which increase the cluster size increasing the entropy, and relax the pre stretched polymer chains decreasing the elastic energy.	An increase in the attractive forces, holding the fixed anions closer to each others decreasing the entropy,and increasing the elastic energy of the polymer.
Water inside the clusters, which is a dielectric material, tends to reorient under the application of electric field; decreasing the effective permittivity of the clusters, reducing the electrostatic repulsive force between the fixed anions.	On the Cathode side this decrease in the effective permittivity of the clusters, increase the electrostatic force between the cations and the anions.
During their migration, the cations will carry some water with them, decreasing the volume of the clusters	This increase in water inside the clusters on the Cathode side, increase the volume of the clusters.
Decrease in the osmotic pressure inside the clusters	Increase in the osmotic pressure inside the clusters

Table 1.1: Changes on the cathode and the anode of four actuation mechanisms (Bar-Cohen, 2001)

1.2.5 Interesting properties of Ionic polymers

Ionic Polymers are soft actuators that perform large bending and flapping deflections when a small voltage is applied across their thickness. The displacement capabilities are in the order of 2% - 5% (compared to 0.1% - 0.3% for the electroactive ceramics) (Shahinpoor et al., 1998). Moreover those materials are soft, flexible, and mechanical parts free which makes them highly dexterous and robust. Finally ionic polymers are able to operate in harsh cryogenic conditions (suitable for space applications, where they operate on temperatures are as low as -130c and pressure of few Torres.)(Shahinpoor et al., 1998). They are also characterized by low actuation voltage (electric potential) in the order of 1$\tilde{5}$V for the 0.184 mm thickness polymers.(Akle and Leo, 2003) (suitable less than 1.23 V in order to avoid electrolysis.) On the other hand ionic polymers have a number of disadvantages to overcome. A major problem developers faces most of the time when dealing with ionic polymers is that they need to be hydrated all the time to operate properly (this might be an advantage in case of underwater applications, or biomedical application in which they will be implemented inside the hydrated humid human body.) Furthermore, ionic polymers relaxe after they bend due to a step response, and it is believed that this is due to the back diffusion of water (Bar-Cohen, 2001). This property makes it more like a velocity actuator, rather than a position actuator, and the same applies when they are used as sensors (The sensing signal behaves like an impulse, when a step deflection is applied to the polymer.) Finally they are non-linear in there behavior, and time variant, which makes characterization and control difficult.

1.3 Initial Motivation

The initial focus of the thesis was to study the feasibility of using ionic polymers as flapping mechanisms for flapping flight based Micro Air Vehicles (MAV). Flapping flight is a very complex aerodynamic problem which is still under research. Therefore we decided to rely on literature for obtaining some rough numbers Ionic Polymers has to meet in order to fly the MAV. After an elaborate literature survey, a review

paper for Wei Shyy et al. (1999) "Flapping and flexible wings for Biological and micro air vehicles" in the Progress in Aerospace Sciences provided us with those numbers. Comparing the aerodynamic requirements with the experimental data on Ionic Polymers, we realized that single layer ionic polymers are far from being able to fly an MAV. The major difficulty was the small force Ionic Polymers can generate, thus the focus went on increasing it. At first we explored the possibility of increasing the actuation voltage. This attempt went in vein after the ionic polymers reached a saturation voltage and this increase in voltage also induced the electrolysis of water inside the polymers. Thus the option of increasing the voltage was eliminated for water based ionic polymers. Finally we were left with the option of stacking ionic polymers, which proved effective. Furthermore, multilayer ionic polymers proved to solve several problems related to ionic polymers and their applications. Therefore, we changed the aim of this thesis toward characterizing and improving the stacking of ionic polymers.

1.3.1 Potential applications

All the interesting properties mentioned in the previous section gives ionic polymers a number of potential applications. Those applications can range from using them as sensors or as actuators. They could be used in water submerged applications, or in other environments either as packaged polymers or ionic liquid solvent based polymers (Bennett and Leo, 2003). Ionic polymers are usually made in the form of thin plates (50 184 micrometer) enabling them to be use in MEMS (Micro Electro-Mechanical System). They might be used as sensors to create micro-accelerometers, or as actuators to create micro swimming robots. Another interesting property of ionic polymers is that they are not toxic for human since they are made of Nafion^{TM}, noble metals (Platinum, and Gold for the coating), and Li or Na ions. This makes it possible for them to be implemented inside the body. Application can range from health monitoring as pressure and pulse sensors, or as active veins as actuators. A current application under research by our group, is using those transducers to detect acoustic signals generated by the turbulance induced by a stenosis (artery closure).

Detecting and characterizing this turbulance enables us to measure the severity of the closure. The end product of this research is a non-invasive ionic transducer device capable of detecting early stenosis. As actuators Matt Bennett in our team is trying to create an adaptive miror for outer space applications. The polymers will be plated with a reflective material, and the potential applied across the transducers will deform the shape of the miror increasing or decreasing the convexity. Furthermore, ionic polymer mechanical properties are quite similar to the human muscle, which raise there potential of replacing Human muscle. Shahinpoor et al. (1998).

Their high dexterity makes them perfect for robotics applications, they can be used to build end-effectors as dexterous as the human hand or as soft malleable end-effectors

Moreover this thesis has focused on two potential applications for the ionic polymers. Due to their mechanical similarities to biological muscles and their large flapping displacement capabilities we were interested in studying the possibility of their use in flapping Micro Air Vehicle (MAV) application, as engines, controllers and sensors. As for the combined sensors-actuators stack, we gave attention to their application as soft, large displacement micropositioner.

1.4 Overview of Thesis

1.4.1 Research Objectives

The objective of this thesis is to build and characterize multilayer ionic transducers. Ionic actuators generate small forces on the order of 0.5mN for a 22mm*5mm*0.2mm beam. The operation of those transducers depends on the mobility of ions inside the polymer clusters. A solvent is required for ions to move, and those solvents have a certain electrical stability window. For water this stability window is around 1.2V; the voltage at which water starts to decay into hydrogen and oxygen gases (electrolysis). Parallel multilayer stacks are developed to minimized the electric field requirements for actuation, and therfore increasing the force per unit voltage. The mechanical con-

straint at the interface is proven to provide a tradeo- between deflection and force. Characterizing this interfacial friction provides designers a controllable parameter for their application. In order to model the interfacial friction in multilayer transducers, a Finite Element Analysis (FEA) method capable of modeling their mechanical structure is developed.

Moreover, combined multilayer stacks are developed for use in feedback control. They are fabricated as an ionic sensor embedded inside a multilayer ionic actuator. The combined multilayer transducers o-ers a compact sensor-actuator that will be used in precision applications.

Another objective was to develope a modeling tool capable of representing multilayer polymers as transducers. Newbury's equivalent circuit model is modified to accommodate the multilayer polymers. The modification is performed on four di-erent boundary conditions, two electrical: series and parallel connection; and two mechanical: zero interfacial friction and zero slip on the interface.

1.4.2 Contribution

The main contribution of this research is the development and characterization of a stacking process for ionic polymer materials. In order to characterize the stacking, we measured the free displacement, blocked force, transfer function, resonance peaks, and the sensitivity for di-erent stacking techniques and di-erent number of stacks. During the characterization process we realized that the free displacement could be controlled by controlling the interfacial slip between the ionic polymer layers. If there is no slip the stack will behave as if it was one complete block, thus the natural frequencies will increase, while the free displacement will be reduced. On the contrary if there is no friction between the faces, both the natural frequencies and the free displacement will be preserved. As for the blocked force, it increased with the number of layers for the parallel stacking, while it remained approximately the same for series stacking. In sensing, it was found that those polymers acts as charge generators and since we were measuring the short circuit current amplifiers, we found that parallel stacking increases the sensitivity proportional to the number of stacks, while in the series

stacking it remained constant. As for the combined sensor-actuator stack, the major problem was to eliminate the feed-through. Feedthrough is defined as the portion of the actuating signal of the adjacent ionic polymer that is directly fed through to the output signal of the sensor. The feed-through was mainly due the humidity in the gaps between stacks which created a short-circuit between the sensor and the actuator(s).

Newbury's equivalent circuit representation of ionic polymers was modified to accommodate the multilayer polymers. The modification was performed on four different boundary conditions, two electrical (series and the parallel connection) and two mechanical (zero interfacial friction and zero slip on the interface). This modified model has the ability to model cantilever multilayer ionic transducers as sensors and actuators. It provides a transfer function that could be used in control, and system level design of ionic transducer devices.

By using the FEA method and stacking technique we were able to design two different MAV wings. The first wing was design to be fully made of ionic polymer sheets. It was designed as a semicircular wing to make the best use of the area covered (keeping the size of the MAV as small as possible). While the second wing was developed and was composed of two different materials: the passive light material that forms the wing surface, and a stack of 10 ionic polymer sheets of 7 x 5 cm size that performed as muscles to actuate the wing.

Finally this whole research could evolve into a project of larger scope to develop micro-layered ionic polymers stacks, that could perform much better than the single ionic polymers sheets. These stacks will provide higher forces, while their free displacement and resonance could be controlled by the manufacturing process, moreover we might be able to integrate some sensor layers for feedback control, which in turn will be able to reduce or eliminate the slow relaxation and high overshoot which characterize ionic polymers.

1.4.3 Approach

Chapter 2 provides an overview for the five different characterization tests we perform in order to characterize ionic transducers. The output of those tests are described, and a description of the two test setups with all there parts is presented.

Chapter 3 is devoted for the characterization of Ionic polymer stacks. At first an explanation of the parallel and series stacking techniques is presented, and a comparison between them is also provided. Than both series and parallel stacks are characterized as sensor stacks and actuator stacks in two different sections. Characterized was the free displacement and blocked force, for a step response, and as a transfer function. Finally a FEA method was provided, verified, and used to simulate the behavior of the stacks.

Chapter 4 introduces the combined sensors-actuators, explores its potential applications and importance. This chapter will discuss the manufacturing techniques, which focuses on the electrical connections and insulations. It also elaborates on the signal feed-through problem. Finally it will explore the Laplace domain model which could be used in control applications.

Chapter 5 modifies Newbury's model to accommodate the multilayer polymers. The modification was performed on four different boundary conditions, two electrical the series and the parallel connection, and two mechanical the zero interfacial friction and the zero slip on the interface. Finally experimental results on transducers with one to four layers are performed and the results are compared to the new modified equivalent circuit model.

Chapter 6 is devoted to the final design of the Micro Air Vehicle (MAV). It illustrates the requirements provided by the review paper previously cited. Furthermore two Finite Element designs will be demonstrated and explained. And finally a summary with conclusions and propositions for future work are presented in the last section.

At last, Chapter 7 provided a brief overview of the thesis. It also provided our contribution to the field, with conclusions being drawn. And finally, future work was

proposed.

Chapter 2

Experimental Setup

2.1 Introduction

In this chapter a description of the ionic polymer testing experiments with their fixtures and circuits is presented. Five experiments are usually performed in order to fully characterize the transducer. The experiments are the electrical impedance, mechanical impedance, sensor sensitivity, blocked force, and free displacement tests. Each experiment is run using a step input or a random input. The five tests are first described, with details on the circuitry and equipment used. In the last section the output of the experiments are elaborated.

2.2 Experiments Output

Each experiment is run with two types of inputs, a step or a random input. The step input is used to determine the low frequency response (DC) of the transducer. As for the random input, it is usually a white noise with an evenly distributed frequency spectrum applied to the polymer. This test is not analyzed in the time domain; rather it is transformed to the frequency domain using the Fourier transformation. The output of this test is a Frequency Response Function (FRF), which is the magnitude and phase of the output as a function of frequency. The duration of the test is a function of three variables; it is inversely proportional to the sampling rate, proportional to the

number of data points per frame, and proportional to the number of averages taken. The sampling rate F_s determines the frequency range of the FRF. Ideally the range of the FRF extends to $\frac{F_s}{2}$, but due to the incorporation of anti-aliasing filters around 28% of this range are eliminated. The number of points per frame N_p determines the resolution of the FRF which is equal to $\frac{F_s}{N_p}$. Several frames of data are gathered and the resulting FRFs are averaged to obtain the final FRF. The FRFs of each frame are compared together and a coherence function is computed. When the FRFs are identical the coherence is one, and if they are totally dissimilar the coherence is zero. Ideally for a causal system the coherence should be one, but noise and some other sampling effects ruins it by introducing random data to the output or input of the system or both. A low coherence means a small signal to noise ratio. Finally a window function is usually multiplied by each frame for before processing. In this thesis the popular Hanning window was used throughout. The role of the Hanning window is to reduce the leakage due to sampling, reduce the effect of the uncorrelated content in the beginning and the end of the frame due to phase shift.

2.3 Types of Experiments

The five different experiments are explained in this section. Both impedance tests are conventional to any material, while the electromechanically coupled experiments are customized for ionic polymers.

2.3.1 Electrical Impedance

Electrical impedance is defined as electrical resistivity and capacitance of the transducer. Therefore the output of this experiment is a tranfer function for the resistance and capacitance of the ionic transducer.

The experiment starts with applying a known voltage across the ionic polymer while measuring the open circuit current. The current measuring circuit is shown in Figure 2.1. The electrical impedance is the known voltage (V) applied divided by the

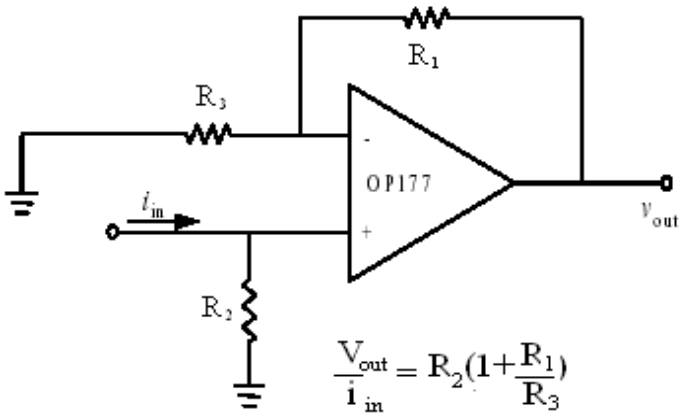

Figure 2.1: Schematic drawing showing the experimental setup for the blocked force test.

current sensed (I).

$$Z_E = \frac{V}{I} \tag{2.1}$$

The resistivity is the real part of the impedance, while the capacitance is the imaginary part.

2.3.2 Mechanical Impedance

Ionic polymers are considered viscoelastic materials that are modeled using two mechanical impedance terms. The first term is the static modulus, while the second is a frequency dependent term. Newbury and Leo (2002) have used the GHM method to simulate the frequency dependent term.

A schematic of the setup used in this experiment is shown Figure 2.2. The shaker applies a mechanical deformation while the linear potentiometer measures the displacement (D) and the load cell measures force (F). The mechanical impedance is

$$Z_M = \frac{F}{D} \tag{2.2}$$

The testing configuration used in this fixture is valid for low-frequency measurement. This was shown by John Franklin in the CIMSS, but this configuration is handful for the next test.

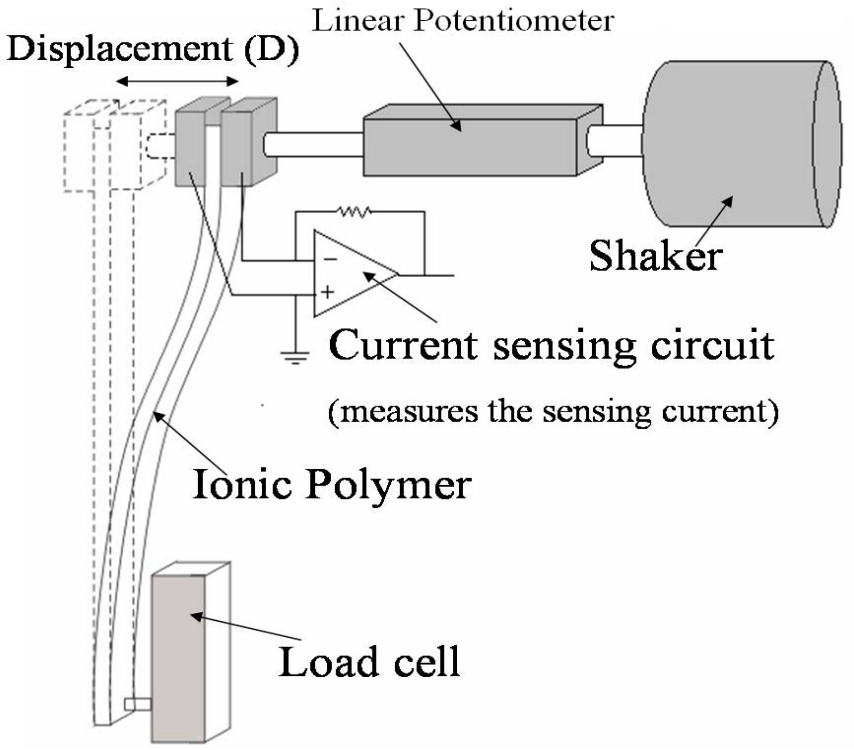

Figure 2.2: Schematic drawing showing the experimental setup for the blocked force test.

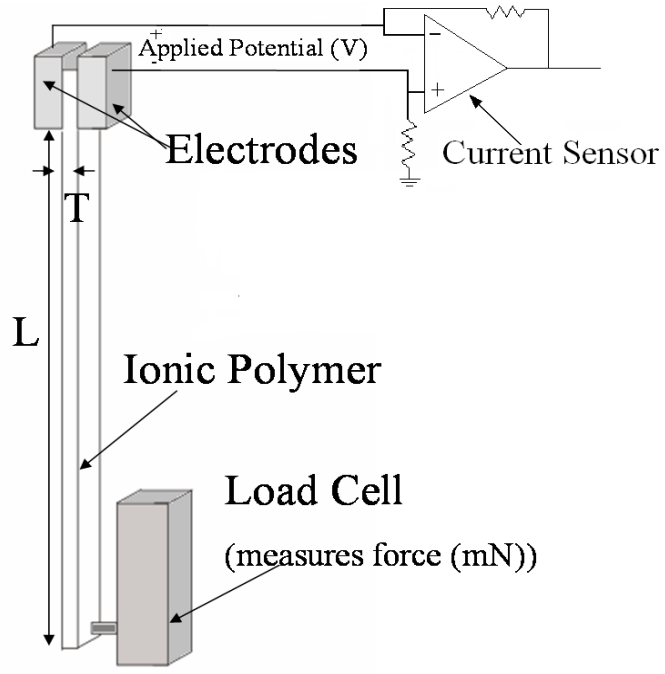

Figure 2.3: Schematic drawing showing the experimental setup for the blocked force test.

2.3.3 Sensor Sensitivity

The setup shown in Figure 2.2 is also used to determine the sensor sensitivity of the ionic transducers. The shaker is applying the mechanical deformation, but instead of measuring the load at the tip a short circuit current sensor is measuring current formed due to the applied strain. The sensor sensitivity of ionic polymers is measured either as a charge or a current (S). A voltage sensor provides less sensitivity since those transducers are highly capacitive (Newbury, 2002). The sensitivity is measured as

$$\text{Sensitivity} = \frac{S}{D} \tag{2.3}$$

2.3.4 Blocked Force

In this experiment the polymer is connected to a power supply, and it is actuated with a known applied voltage (V) on the electrodes. On the other side, a load cell is blocking the motion of the polymer and measuring the force generated (F). The setup is shown in Figure 2.3. The blocked force is the maximum force this polymer

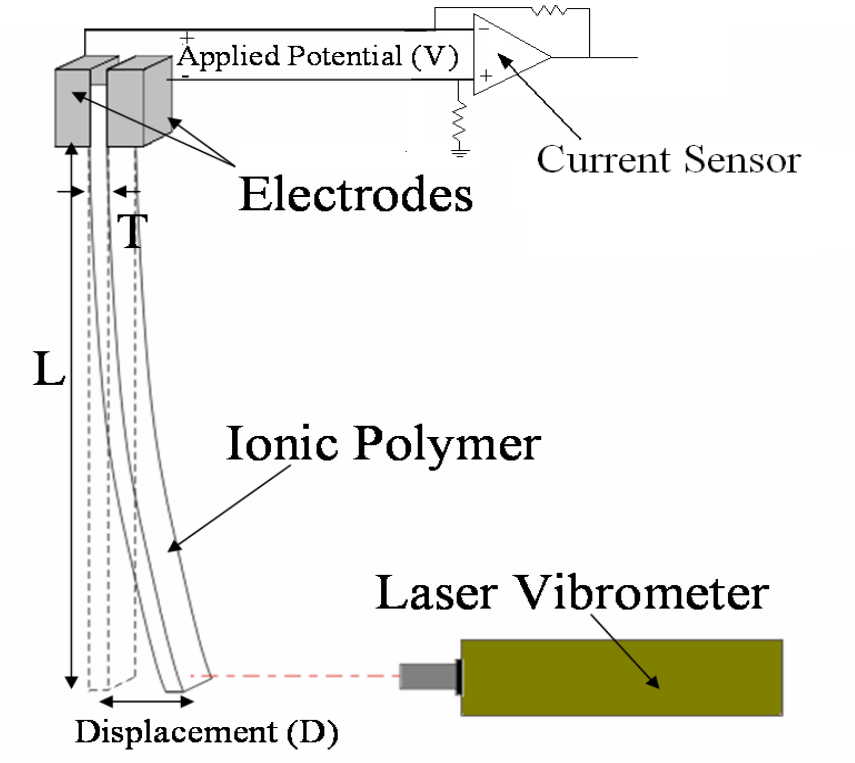

Figure 2.4: Schematic drawing showing the experimental setup for the blocked force test.

can generate and computed as follows:

$$\text{Blocked force} = \frac{F}{V} \tag{2.4}$$

2.3.5 Free displacement

The free displacement experiment is another actuation experiment, but it differs from the blocked force test by the mechanical boundary condition.

The experimental setup is shown in Figure 2.4. A known voltage (V) is applied to the polymer, while a laser vibrometer measures the transducers tip displacement (D) without adding any obstacle to the free motion. The free displacement is:

$$\text{Free displacement} = \frac{D}{V} \tag{2.5}$$

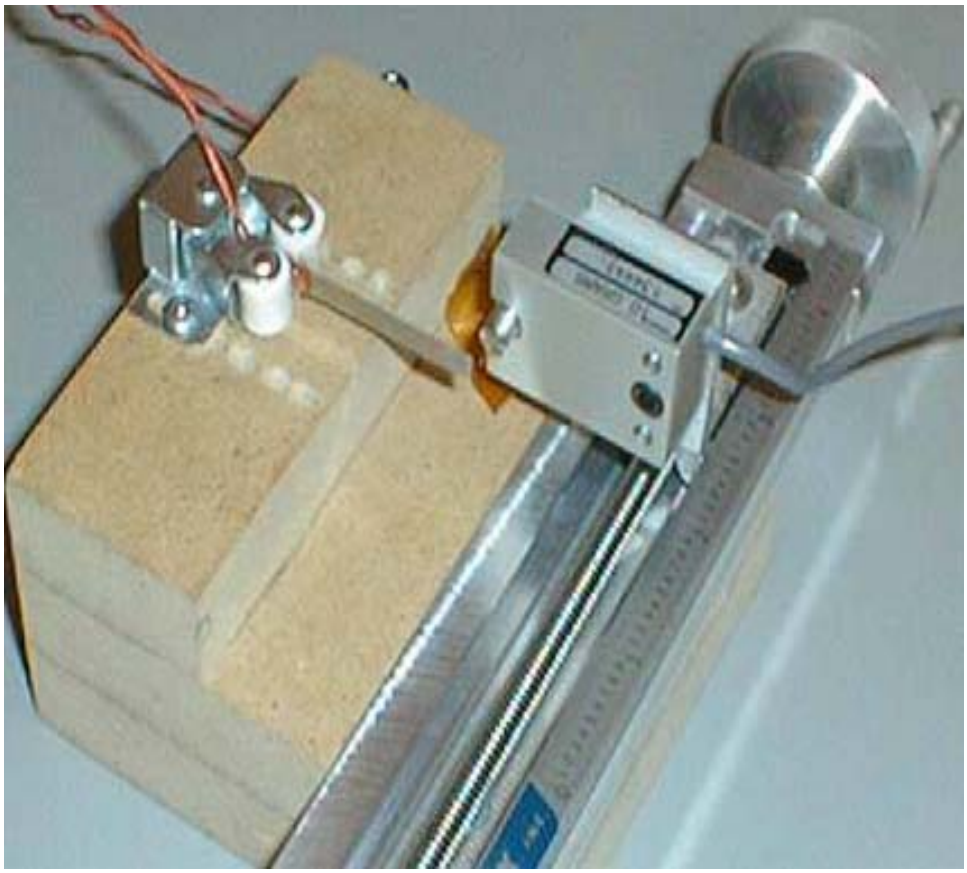

Figure 2.5: Fixture 1.

2.4 Equipment Description

In the five previously described experiments ionic polymers were clamped at one end with two gold electrodes. All the experiments are conducted in air, and deionized water was brushed on polymer approximately once a minute. This insured that the hydration level is kept within an acceptable range. When not in use, the transducers were stored in deionized water.

Two test fixtures were used the experiments in this thesis. Fixture 1 was acquired from previous researchers in the CIMSS lab Newbury (2002) and shown in Figure 2.5. It is composed of two separate apparatus to perform all the five tests. The sensing and modulus test was performed on the fixture with the APS Dynamics APS 113 long stroke shaker, which provides large displacement up to 50 Hz. The displacement is measured with a Novotechnik T25 Linear potentiometer and an ap-

propriate circuit conditioning circuit. The signal amplifiers used for characterizing the performance of the stacks is a current amplifier of 10^5 V/amp sensitivity, with the schematics shown in Figure 2.2. Manufacture's specifications of the linear potentiometer indicate a repeatability of 0.002mm and a linearity of 0.06mm. For the modulus test a Transducer Techniques GSO-10 10 gram load cell was mounted on the shaker armature and used to measure the force due to the deformation of the polymer. This load cell was used with a TMO-1 signal conditioning circuit. Its precision, repeatability and linearity were 0.02mN. The GSO-10 load cell was also used to measure the blocked force on the actuation apparatus. The actuation apparatus is shown in Figure 2.5 and is composed of the load cell on a variable cursor so that it is easy to change the boundary condition from blocked force to free displacement. For the free displacement a Polytec OFV-303 laser vibrometer head with OFV-3001 controller and OVD-20 demodulator was used. The resolution of this setup was 5μm. The laser vibrometer was used for frequency response, and small displacement step responses due to its high resolution. But in case a large tip displacement is expected a RedLake imaging Motion Scope PCI 2000 S high frequency digital video camera was used to measure the deformation. This camera could capture video with a rate up to 2000Hz. Image Express MotionTrace image analysis software was used to track the transducer's tip, and generate a tip displacement plot as a function of time. The resolution of the trace software depends on the image quality and the focal length used. It could locate a point within a resolution of a tenth of a pixel. A pixel in our experiments corresponds to approximately 0.1mm.

The second fixture was recently built by members of the CIMSS lab. It is shown in Figure 2.6 with all the components. The load cell and the linear potentiometer are the same ones used in the old fixture. This fixture is built to automate four of the five experiments: blocked force, electrical impedance, mechanical impedance, and sensing sensitivity. Those five experiments are sufficient to fully characterize the polymer. The shaker used in this fixture is a Bruel & Kjaer Instruments shaker, it is capable of higher frequencies (up to 2-3KHz) than the previous shakers. As for the signal processing, we used two digital signal processes. The Tektronix FFT analyzer with

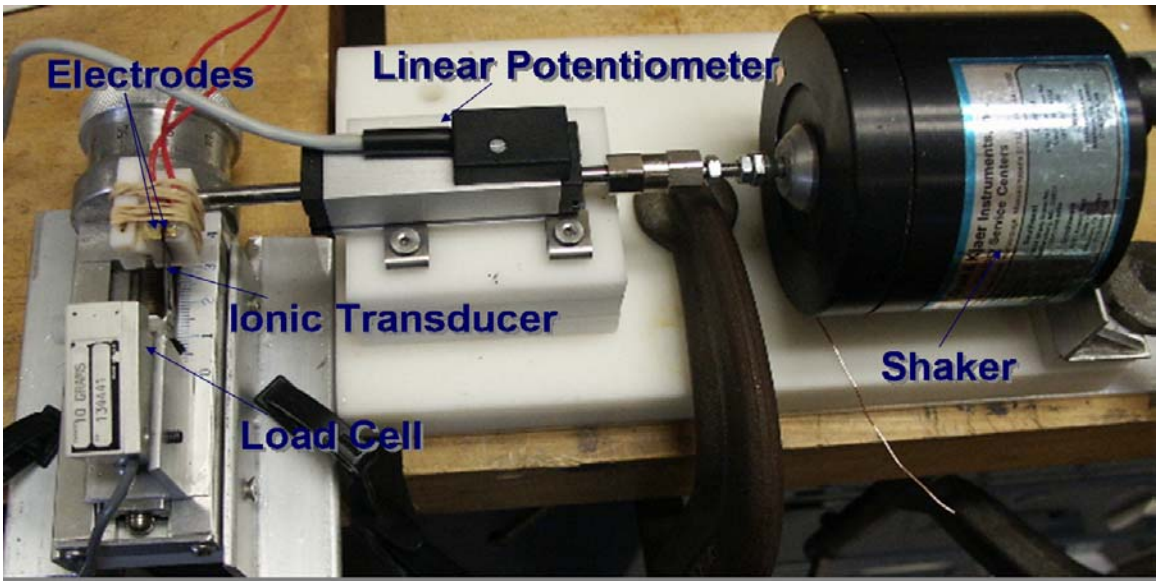

Figure 2.6: A picture showing the new fixture with details on the parts.

a signal generator was used for the frequency response function. A dSpace DS1102 DSP was used to measure the step response.

Chapter 3

Characterization of Ionic Polymer Stacks

3.1 Introduction

As defined in the introduction, ionic polymers are soft actuators that perform large bending and flapping deflections when a small voltage is applied across their thickness. Their major disadvantage is the low forces they apply. To overcome this problem stacking was proposed. In this chapter stacking is thoroughly explained. Parallel and series stacking techniques are explained, and their use as sensors and actuators is discussed. Actuator stacking is performed to determine how interfacial friction affects the free displacement and the natural frequencies. Finally a Finite Element Analysis method will be explained, verified, and used to analyze the experimental results.

3.2 Stacking techniques

As previously mentioned two stacking techniques will be explored: series and parallel. Those techniques are the same mechanically but differ in their electrical characteristics. In the next paragraphs the series and parallel stacking will be explained and a comparison will be provided.

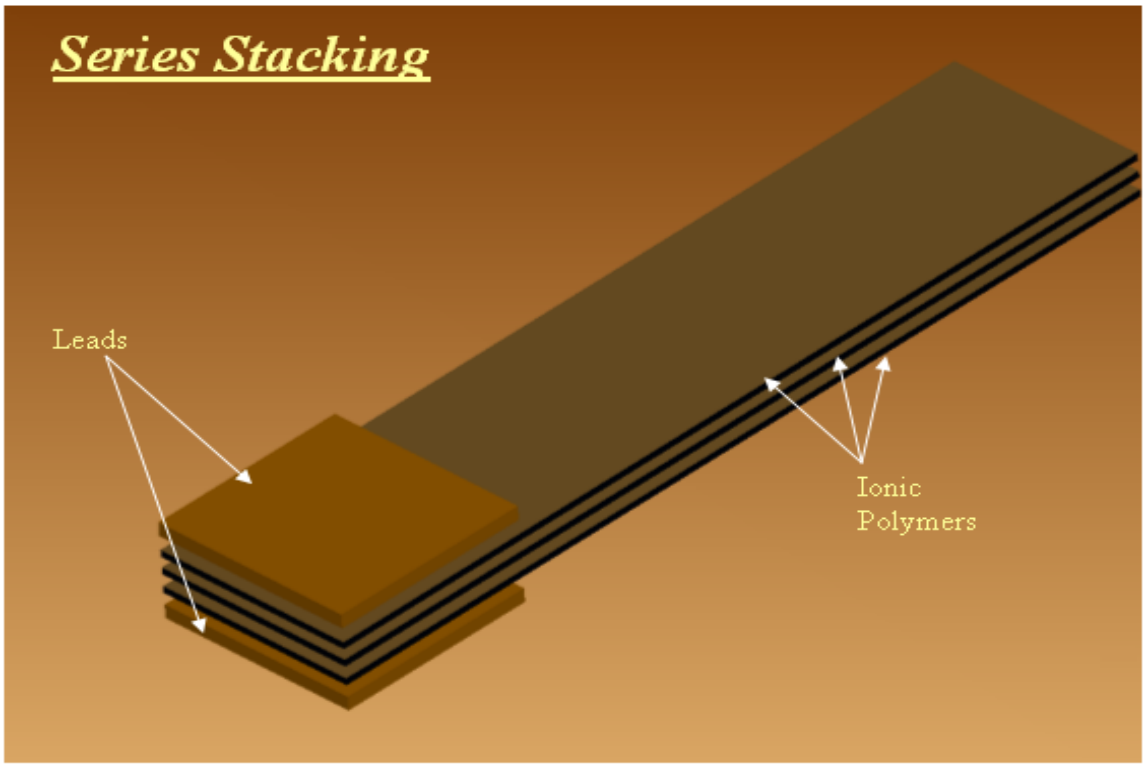

Figure 3.1: A CAD drawing showing the different parts of a series stack.

3.2.1 Series stacking

Series stacking consists of overlaying the ionic polymer sheets on top of each others as shown in Figure 3.1 and providing the voltage V_{total} across the whole stack as shown in Figure 3.2. Assuming that the polymers are of the same size and same electrical impedance,

$$V_1 = V_2 = \ = V_n = \frac{V_{total}}{n}. \tag{3.1}$$

While from the mechanical perspective, the force generated by the separate polymers will be added. As for the free-displacement, and resonance frequency, it will depend upon the interfacial friction, as will be discussed later.

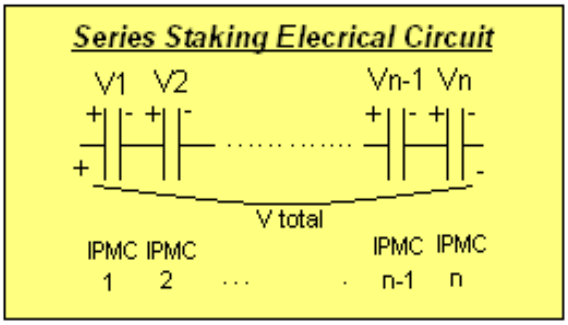

Figure 3.2: Schematic representation of the electric connection for a series stack.

3.2.2 Parallel stacking

Parallel stacking is similar to series stacking, with the only difference is that each polymer will receive a voltage equal to the overall stack voltage:

$$V_{total} = V_1 = V_2 = \ = V_{n-1} = V_n$$

The mechanical connections are shown in figure 3.3, while the electrical connections are shown in Figure 3.4. The fabrication process is illustrated in Figure 3.5.

For the purpose of this thesis, the stacks were layered by hand. The connection leads are made of 3M adhesive copper tapes and Saran Wrap was used for the reported results as insulation material.

3.2.3 Comparison

The main advantages of series stacking as compared to parallel stacking are the manufacturing simplicity, reliability, and the low actuation current. As mentioned before series stacking is simply laying the polymer sheets on top of each other and applying the potential across the whole stack, while the parallel stack requires weaving the leads from one face to the other and adding insulation as elaborated in Figure 3.5. This is a very delicate and tedious process, for example layering a 3 layer stack is more than 40 min of work. Moreover out of each 2 or 3 stacks only one will work properly, because the others will have some internal short-circuits through the insulation or across the leads. This short-circuit is also responsible for the short durability

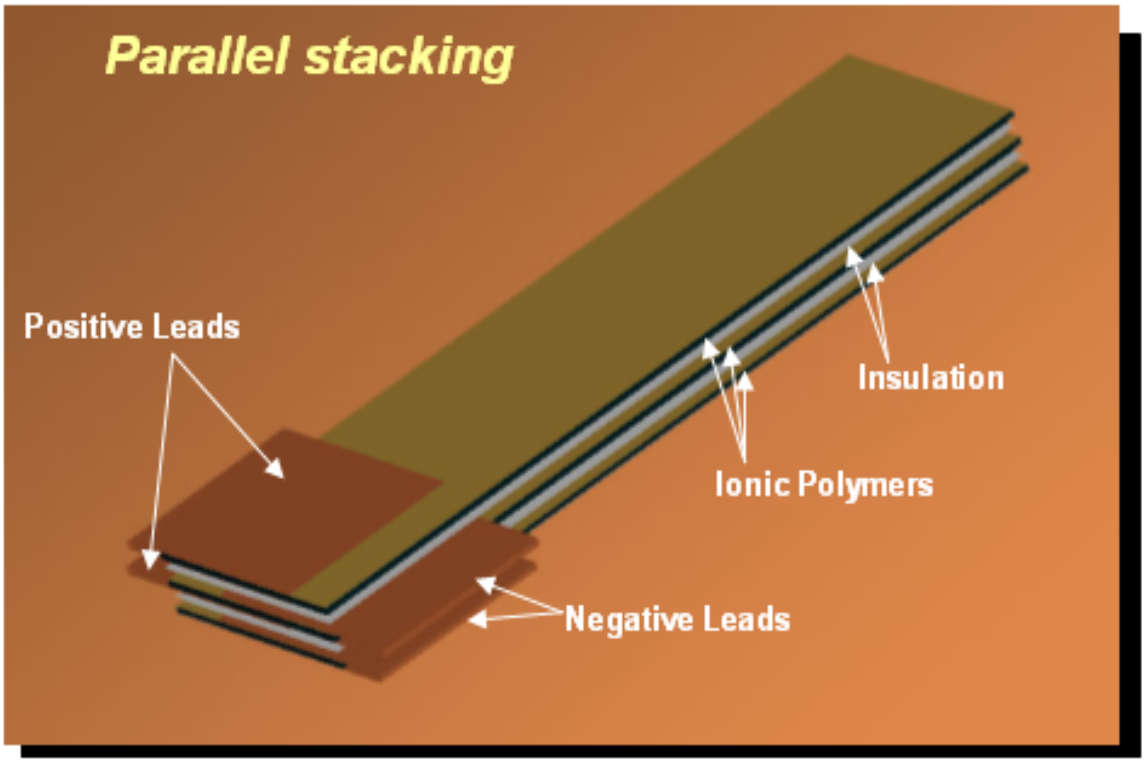

Figure 3.3: A CAD drawing showing the different parts of a parallel stack.

of parallel stacks. Upon usage the insulation might tear, and the leads will make a short-circuit somewhere inside the stack, this small short-circuit will propagate easily and became defective due to the heat it releases, which in turn melts the plastic insulation. Apart from the manufacturing difficulties and short durability problems, parallel stacks are far better in performance than series stacks. They provide low operating voltages, which are the same across each polymer, avoiding the necessity of going to large overall voltages series stacks require; therefore we can safely remain lower than the 1.23V electrolysis voltage limit. In the following sections we will explore the use of stacks as sensors and actuators.

3.3 Sensor Stacks

The first tests investigated the performance and characteristics of series and parallel stacks as sensors. In the first subsection a series and parallel multilayer sensors are compared, and in the next subsection the amplifier was varied and the concept of low

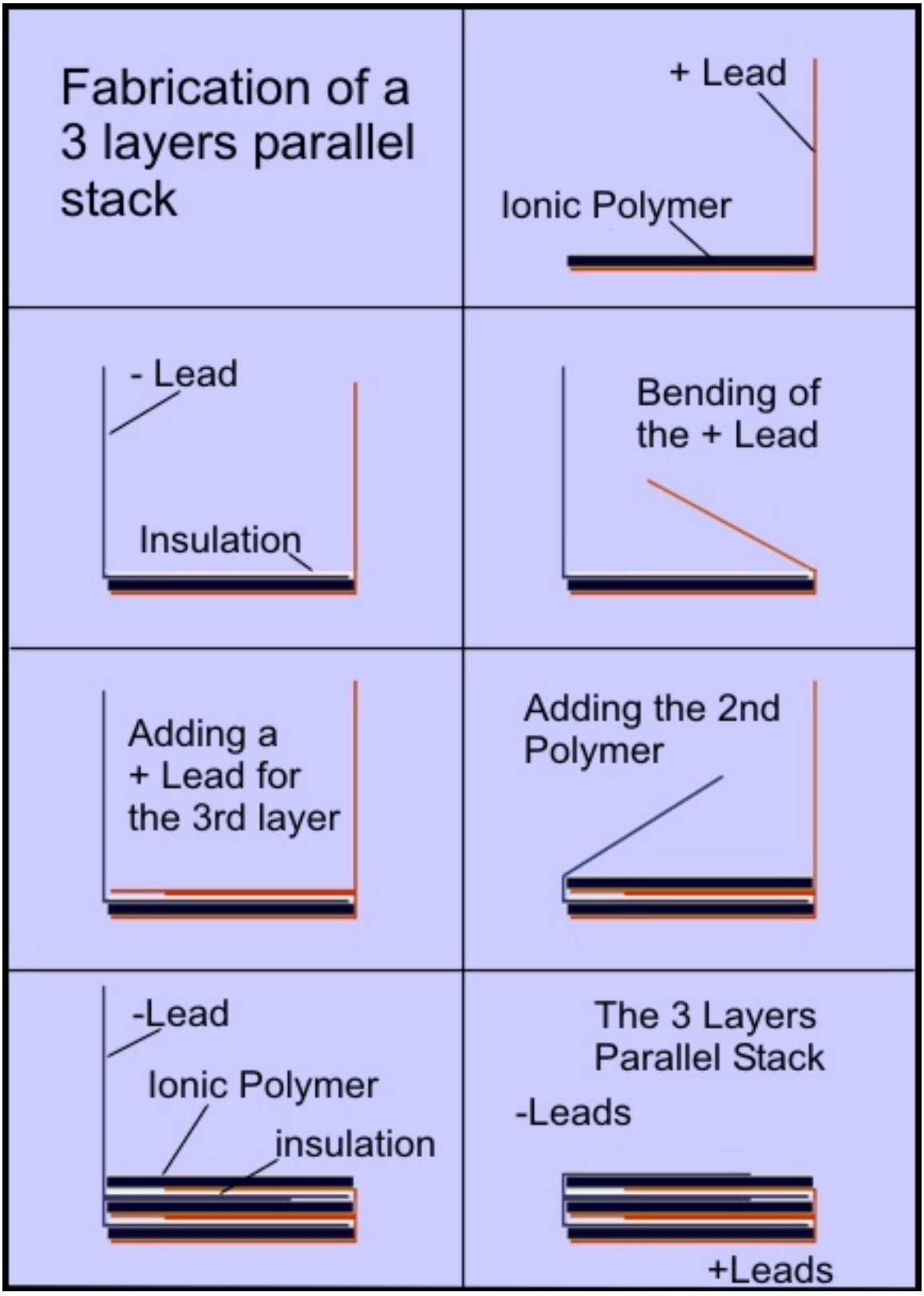

Figure 3.4: Fabrication a 3 layers parallel stack.

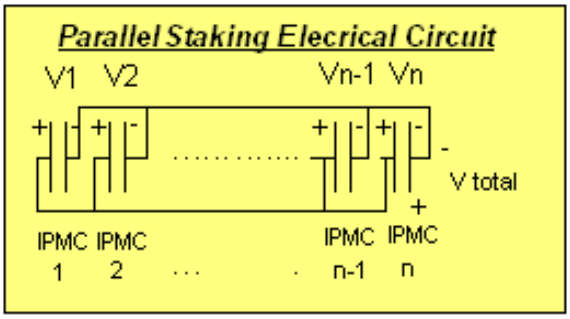

Figure 3.5: Schematic representation of the electric connection for a parallel stack.

pass filtering is explained.

3.3.1 Comparison of Series and Parallel Multilayer Sensors

This section will explore the sensing characteristics of series and parallel stacking. As mentioned before we are using current amplifiers, since according to Newburry ionic transducers perform better when used with a charge amplifier. This is due to their low electrical impedance. Therefore the polymers are seen as current generators, and it is expected that in parallel the current will add, and thus the stack sensitivity will increase proportional to the number of layers. While in series the same current will pass through them all, and therefore it is expected that sensitivity will remain constant. Although Newbury's model (Newbury, 2002) predicted that the sensitivity increase as a function of thickness, series stacks didn't show such a behavior due to the use of current sensing amplifier circuit. In case of a voltage sensing circuit was used (this might happen if the electric impedance of the polymer is changed while trying to enhance it), it is expected that this result will be reversed. Ionic polymers are modeled as a combination of capacitors, and resistors. Thus when added to the amplifier circuit they will act as a low pass filter of approximate cuto frequency

$$t = \frac{1}{RC}$$

where R is the amplifier resistor, and C is the polymers capacitive impedance. (Note that the internal resistor of the polymer is very small compared to the amplifier resistance 1.2Ω compared to $100K\Omega$). Adding the polymers in parallel will increase their

capacitive impedance proportional to the number of layers and the cutoff frequency will be reduced. For this reason we tried to explore new amplifier circuits as discussed in the next section. Figure 3.6 shows the sensitivity ($\frac{\mu Amp}{\frac{mm}{s}}$) increases proportional to the number of parallel layers. Also shown is the decrease in the phase shift due to the increase in the capacitive impedance of the stack which is proportional to the number of layers. As for the last graph in Figure 3.6 it shows the slight increase in the coherence, and this is due to the increase in the sensitivity i.e. the signal to noise ratio. As for the irregularity around 9Hz shown in the figure, it might be due to some resonance in the shaker end.

As for series stacking, Figure 3.7 shows a comparison of stacks with different number of layers varied from 1 to 4 layers. Also included is the transfer function of two different single polymer strips, to emphasize the variation between polymer strips, and validate that the sensitivity of the overall stack is the average of each polymer layer. Moreover the phase shift did not vary much, though it increased a little bit. This is expected due to the decrease in the capacitive impedance when the capacitors are put in series, and therfore an increase in the cutoff frequency of the low pass filter. To conclude, parallel stacking had increased sensitivities and decreased the cutoff frequency. While series stacking did not increase the sensitivity as compared to single polymers, but increases the cutoff frquency. We believe that if voltage amplifiers were used, this result would have been inverted.

3.3.2 Amplifier Variation

For the purpose of improving the performance of the amplifier circuit, especially after the noticable increase in phase shift during parallel stacking, several amplifiers were tried. Ideal sensors would have zero phase shift i.e. they will be feeding back real time data without delay. The more phase lag the worse the sensor is, since it is difficult to add phase lead to a system using a controller. Thus the target is to reduce phase lag as much as possible. This could be achieved by increasing the cutoff frequency, which will lead to a decrease in the phase lag at low frequencies. Though several amplifier circuits were tried, like high impedance charge amplifiers and voltage amplifier. The

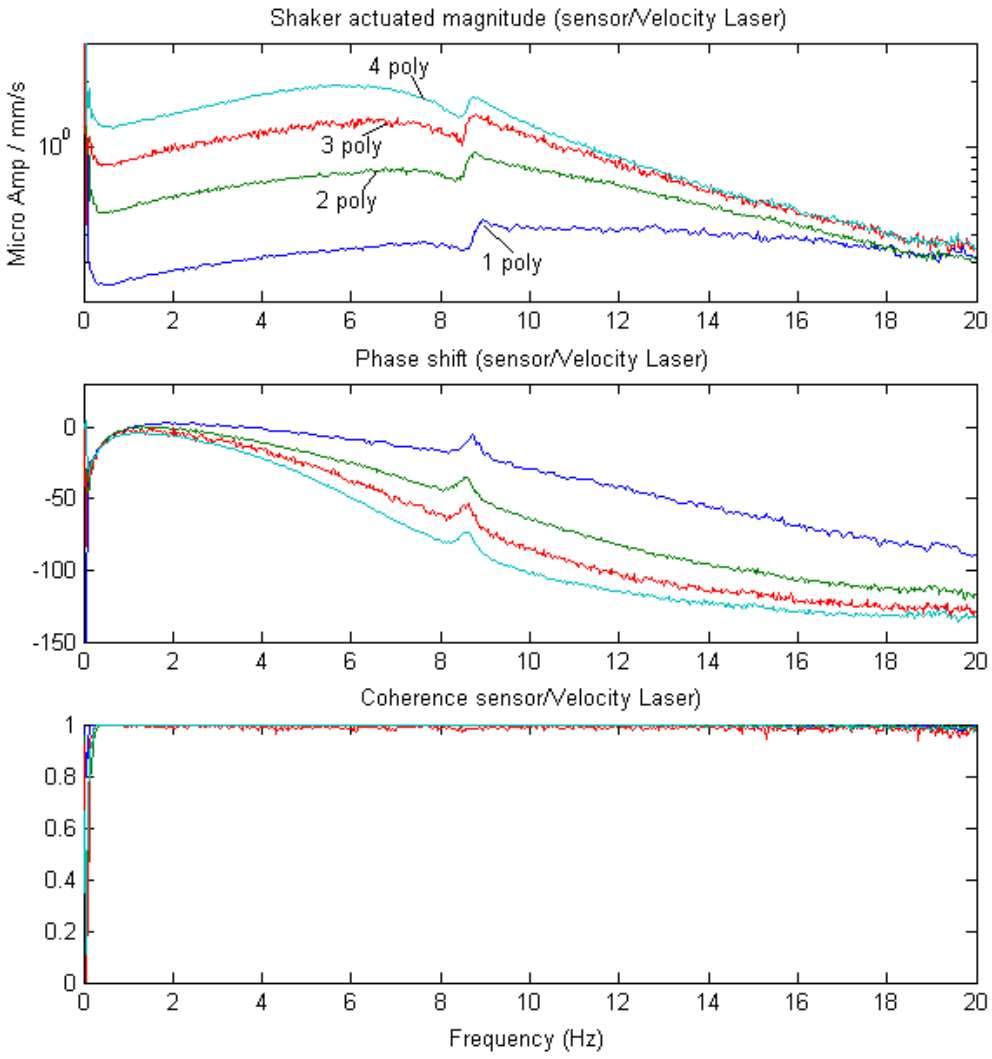

Figure 3.6: The transfer function of parallel stacks with 1, 2, 3, and 4 layers.

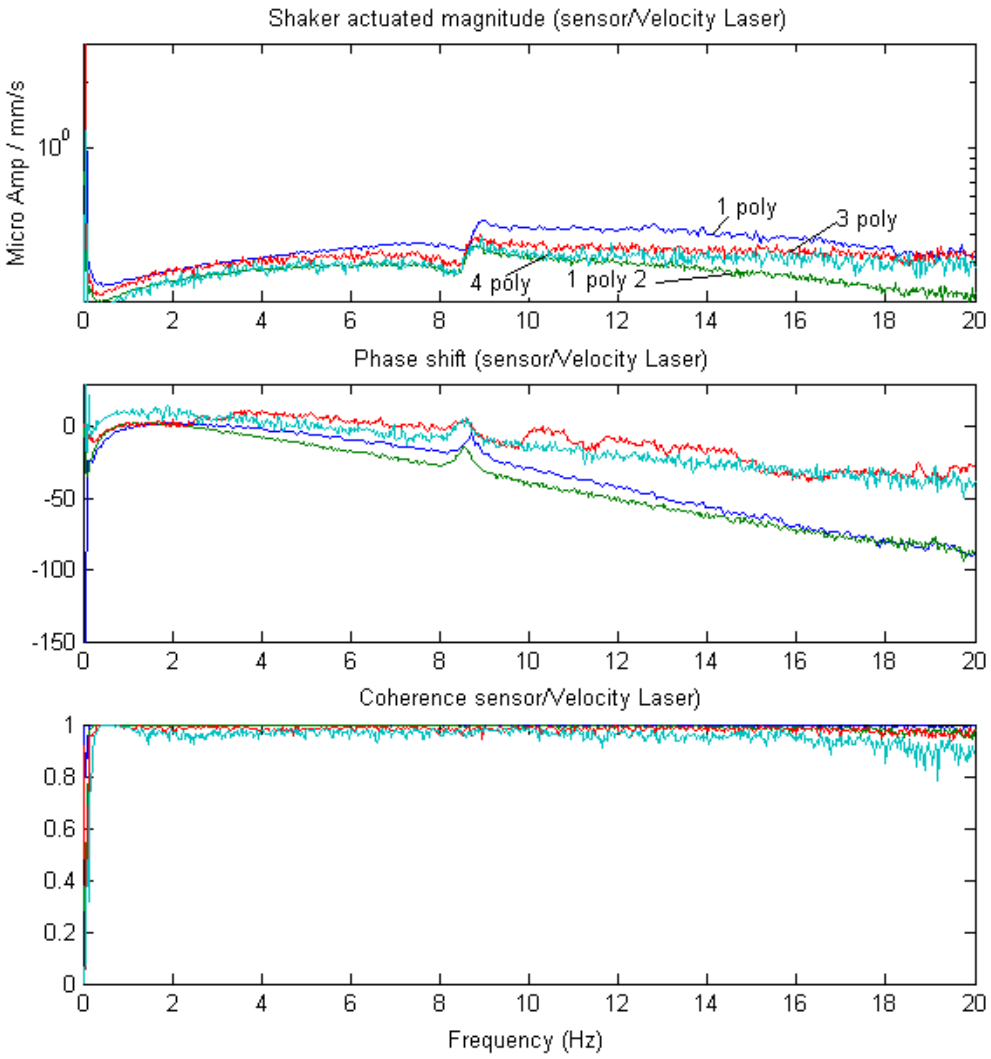

Figure 3.7: The transfer function of series stacks with 3 and 4 layers plotted with two different single layers polymers.

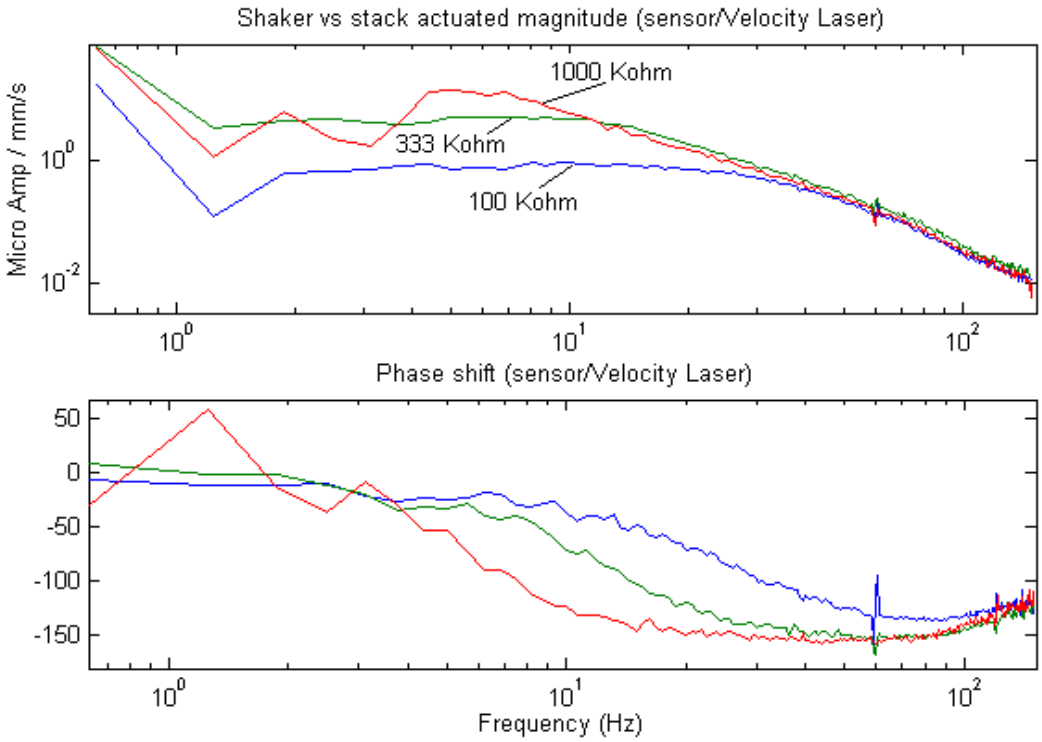

Figure 3.8: Transfer function of the same polymer but with a different value of R_1 in the amplifier circuit

current amplifiers proved to be the only successful ones. The schematic of the current amplifier is shown in the previous chapter in Figure 2.2. Several parameters in this circuit were varied, the first one was R_1, and the result is shown in figure 3.8. The resistance R_1 is a major factor in the cutoff frequency $\tau = \frac{1}{R_1 C}$, and this can be easily verified in figure 3.8. One could see that decreasing R_1 decreases the phase lag at lower frequency, indicating higher cutoff frequency.

The resistance R_2 was also varied to determine its effect on the frequency response. Theoretically, if the Op-amp was ideal this shouldn't have any effect on the response. But as shown in figure 3.9 though the phase shift didn't change, the sensitivity changed dramatically and without any pattern. This weird behavior could be related to the non-ideal behavior of the Op-amp. Moreover, once the amplifier circuit is turned on, a huge DC offset will initiate, but will settle down to somewhere close to zero within 20 to 30 sec. (it could be calibrated to go to zero after those 20

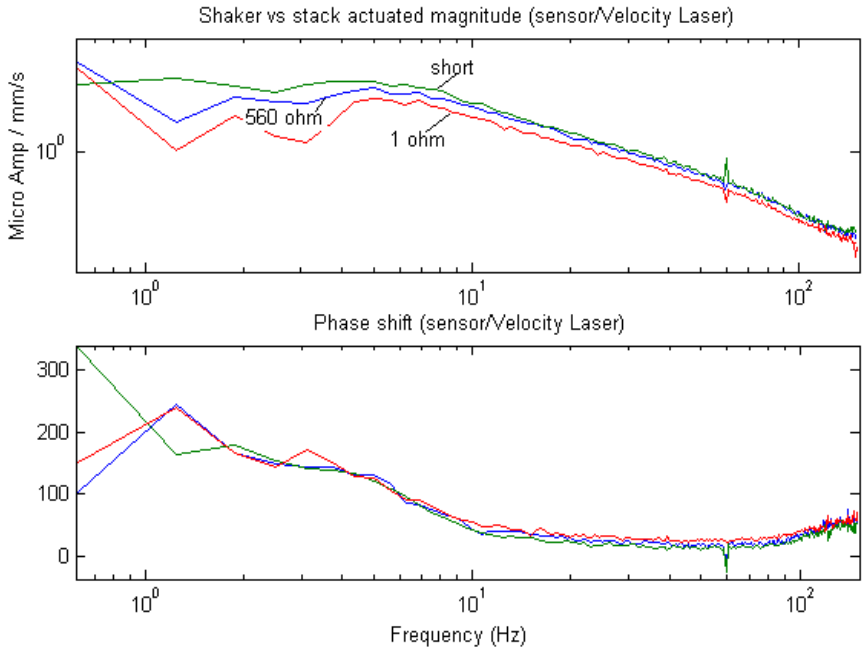

Figure 3.9: Transfer function of the same polymer but with a different value of R_2 in the amplifier circuit

to 30 sec).

By going back to figure 3.8 one can notice that upon decreasing the resistor R_1, the sensitivity of the amplifier is decreasing. Therefore although this was successful in increasing the cutoff frequency, the overall performance of the amplifier was unsatisfactory. Thus it was decided to decrease the resistance R_1, and than use a voltage amplifier, that will simply compensate for the lost in sensitivity without introducing any further phase lag. As shown in figure 3.10 this worked properly, but the only limitation on decreasing a lot R_1, and keep on compensating with voltage amplifier, is that the later amplifier is amplifying both the signal coming out of the sensor, and the noise coming out of the current amplifier circuit. Thus the cleaner the current amplifier circuit is (usually better Op-amps, and better circuit connection.) the more we can make use of this technique, and further increase the cutoff frequency.

As it can be noticed in Figure 3.10, the 10K Ω current amplifier gain resistor (R_1) with 100 times voltage gain amplifier formed the best combination for this technique, it was able to enhance the phase lag by approximately 50 degrees, with

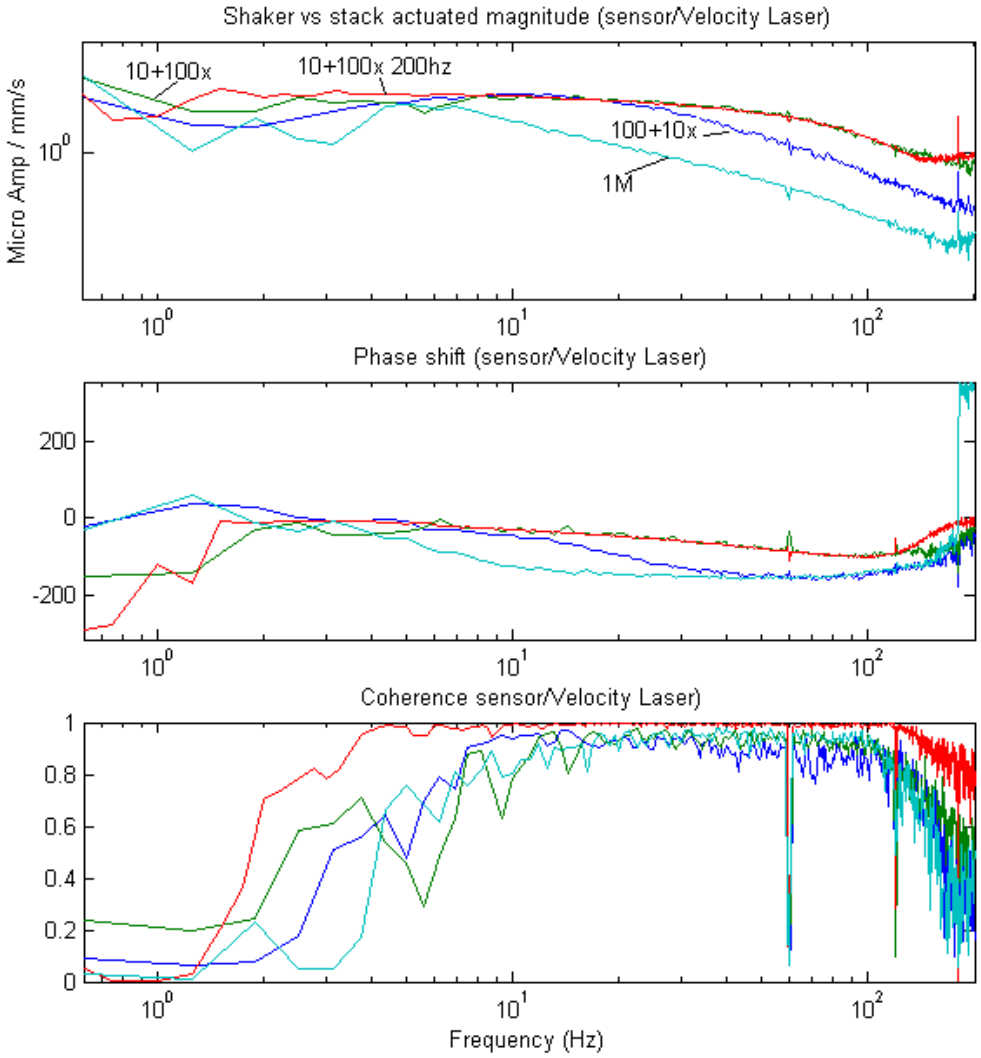

Figure 3.10: Transfer function of the same polymer but with different amplifier circuits

an extended cuto frequency. Going further in decreasing the current amplifier gain resistor, and increasing the voltage gain, would cause high noise to signal ratio and also leading the system to instability. This could be noticed by the increase in the bumps on the 60Hz, 120HZ, and the 180Hz with the decrease in the current gain amplifier and increase in the voltage gain amplifier.

3.4 Actuator Stacks

The main purpose of this research was to increase the force of ionic polymers. The stacks used in this section are the same as the ones used for the sensor analysis. Therefore the manufacturing is identical to what was previously described. In the following sections we will describe the actuation characteristics of the series and parallel stacks, and the role interfacial friction plays in determining those characteristics.

3.4.1 Comparing Series and Parallel Stacks as Actuators

As previously discussed the only difference between the series stacks and parallel stacks is the way the voltage and current are provided to each polymer. Thus if we reduce the analysis to voltage per polymer rather than voltage per stack (i.e. if we apply V to the parallel stack we should apply n*V to the series stack, where n is the number of layers), we should obtain the same output. For this reason all of our results are expressed in terms of voltage per stack, thus the difference between series and parallel would be emphasized. In this section we will discuss the blocked force results. Results for the measurement of free displacement and resonance will be presented later since they are related to the inter-facial friction between the polymer layers.

In this section we will discuss the blocked force results. Blocked force step results are shown in Figure 3.11 for 22mm x 5mm x 0.2mm polymers with different numbers of layers. Measuring the blocked force in ionic polymer one would read the maximum force rather than reading the steady state, because the steady state will go to zero with time due to its inherent relaxation property. Looking at Figure 9 one

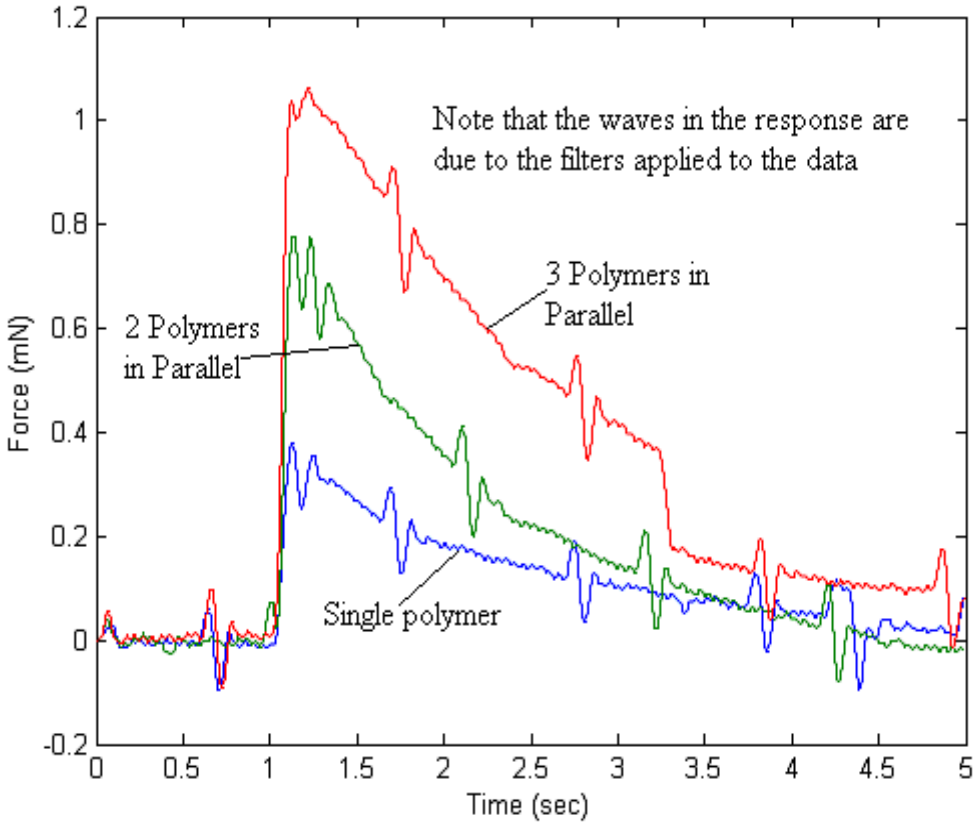

Figure 3.11: The Blocked force step response of the differently layered parallel stacks

can notice that the blocked force has increased from 0.37mN for the single layer to approximately 1.08mN for the three-layer polymer. Considering this result one can deduce that they fit the equation

$$F_{total} = N_L F_{layer} \tag{3.2}$$

where F_{total} is the total output of the stack, F_{layer} is the force output of a single layer, and N_L is the number of layers. The real blocked force will deviate from the value in the equation with the increase of the number of layers in the stack, and this mainly due to two reasons. The first is due to the electric losses in the electrical leads that connect the polymers together, note that this effect can be decreased in case of more accurate layering. The second reason might be due to the damping that the insulation material and the polymers themselves are introducing to the overall system.

Shown in Figure 3.12 is the frequency response function of the blocked force

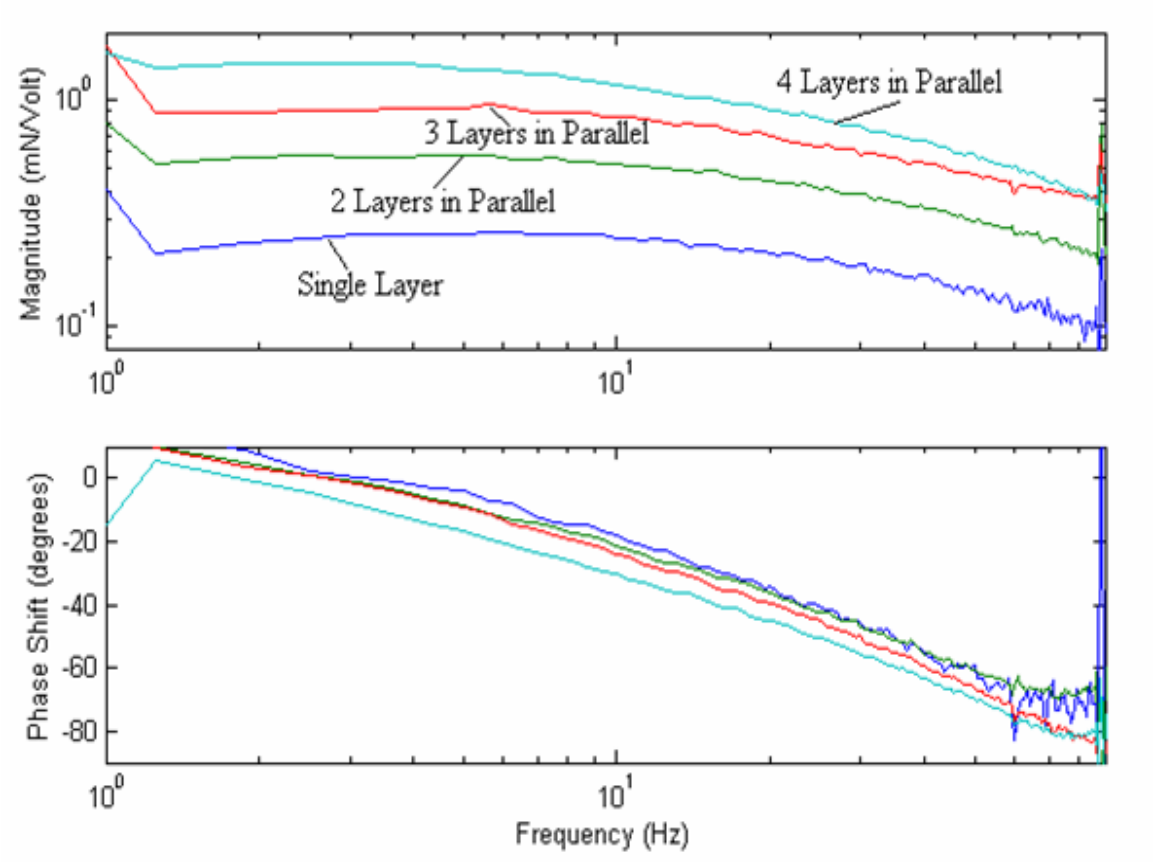

Figure 3.12: The Blocked force transfer function of the differently layered parallel stacks

for a parallel stack with different numbers of layers. It provides more evidence to support equation 3.2. A note is that the y axis in the magnitude plot in this figure is presented in a log scale, thus the distance between the four functions is not equal.

The blocked force of series stacks were characterized in the same manner. Since the voltage per layer will decrease with the addition of more layers (refer to equation 3.1) the force per layer will decrease proportionally, and therefore the addition of layers while holding the overall stack voltage constant will not amplify the force, but it will remain constant, as shown in Figure 3.13. The results shown in Figures 3.11 through 3.13 represent the blocked force boundary condition, while the free displacement boundary condition will be illustrated in the next section which discusses the major parameter in free displacement.

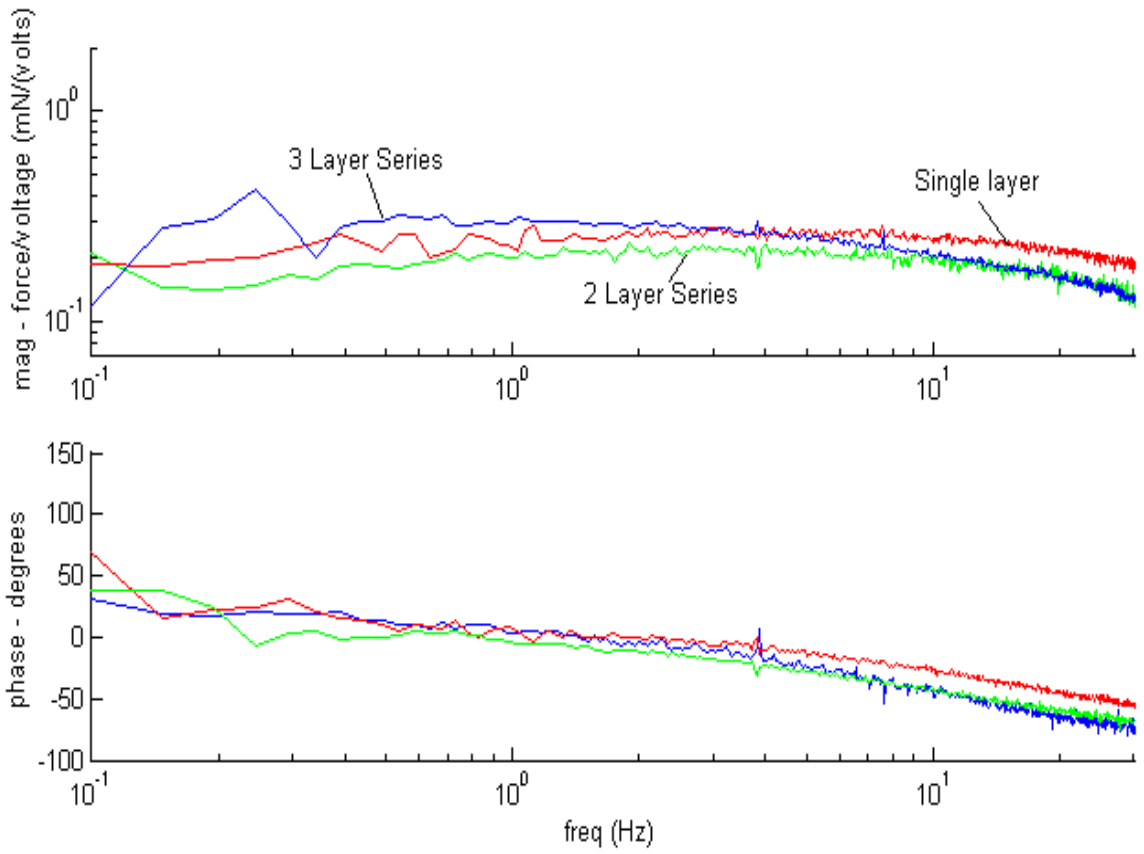

Figure 3.13: The blocked force transfer function of series multilayered actuators

3.4.2 Interfacial Friction and Mechanical Properties

The term inter-facial friction is referred to as the friction between the polymers in the stack. The substantial difference in free displacement between packaged and unpackaged polymer stacks made us realize the importance of inter-facial friction. As described in the introduction, ionic polymers move due to one or several mechanisms which occur inside the polymer.

For modeling purposes, one can look at the bending mechanism (s) as an internal pressure applied to the polymer. This internal pressure will increase proportional to the number of layers, while if considered as one block the stack thickness will also increase proportional to the number of layers. Therefore the number of polymers and the thickness both increase proportional to the number of layers n. The tip displacement of a cantilever beam due to an applied pressure is (Shigley and Mischke,

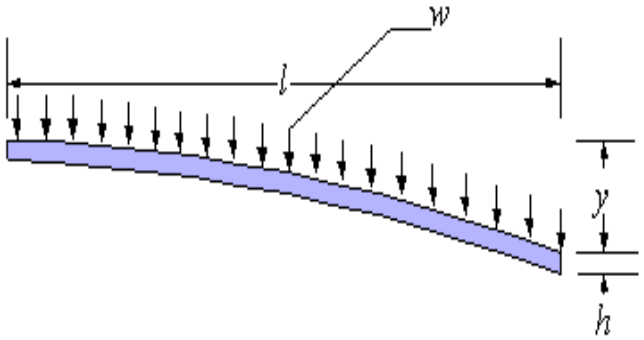

Figure 3.14: A cantilevered beam with an applied pressure w.

1989)

$$y = \frac{wl^3}{8E\left[\frac{bh^3}{12}\right]}, \tag{3.3}$$

where w is the applied pressure, h is the thickness, E is the modulus of elasticity, and is the length as shown in Figure 3.14. Therefore if both w and h are proportional to N_L, y is proportional to $\frac{1}{N_L^2}$. Thus with the increase in number of layers N_L, theoretically the tip displacement or the free displacement will decrease proportional to N_L^2. When the layers are well attached to each other there is high interfacial friction and they will act as a single thick beam. In this case the free displacement will be reduced. While if the inter-facial friction is low, the polymers are sliding freely on each other and they will remain acting as single polymers but with an increased force. The packaged polymer stacks are considered to have higher inter-facial friction; moreover the external package will also block the internal motion of the layer, leading to more beam-like behavior.

As for the unpackaged stacks which we consider as low interfacial friction stack, we used Saran wrap as the insulation layer (which is also responsible for the interfacial friction in the parallel stacks), which is a smooth material especially when wet. Shown in Figure 3.15 is the free displacement step response for unpackaged parallel stacks of 1, 2, 3 and 4 polymer layers. One can notice that the variation in free displacement, which is measured at the peak remained within 10%.

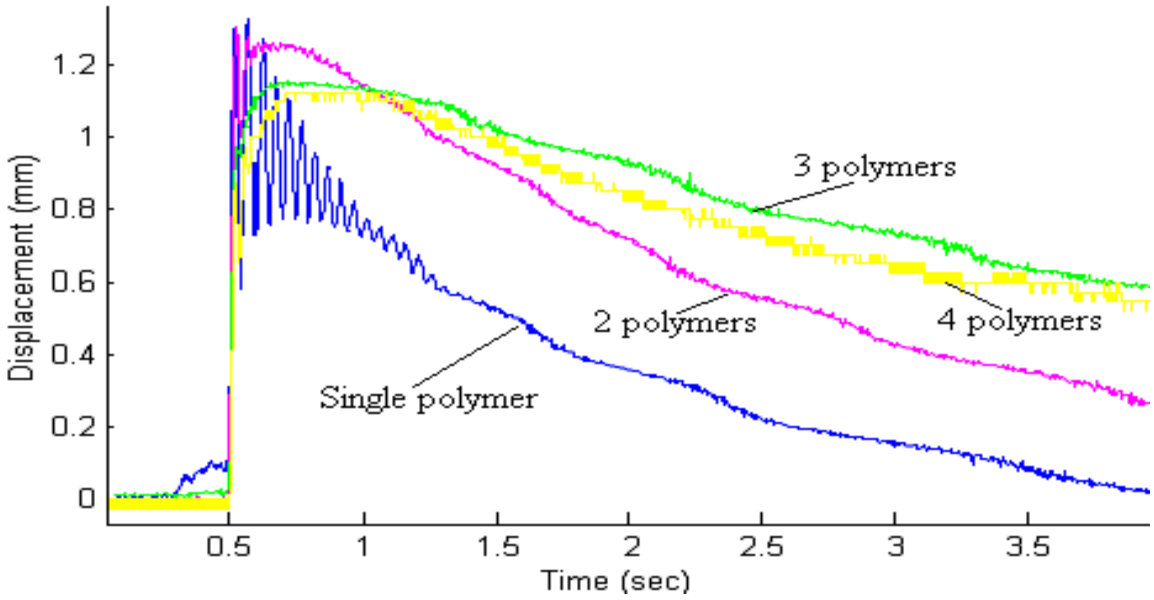

Figure 3.15: Step response for unpackaged parallel stacks

If one looks further in Figure 3.15, it can be noticed that the relaxation speed is quiet different. Though no definite pattern could be noticed, one can infer that with the increase of number of layers, the relaxation is getting slower. This is mainly due to the increased damping of the passive insulation material and the polymers themselves. As for the natural frequencies, it can be seen in Figure 3.16 that the peaks location changed only 26%, indicating that in the ideal situation those frequencies would remain constant. The first mode lies approximately between 19 and 26 Hz range for all the stacks.

In the case of a packaged polymer, the inter-facial forces and the packaging are making the stack act as a unit block. Figure 3.17 shows the unit step response for the packaged polymers. It can be easily noticed that the free displacement decreased as a function of the number of stacks. Figure 3.18 shows the large variation of the natural frequencies which increases with the number of layers, and reach sort of saturation. The displayed data are for the first three natural frequencies. Those data are obtained from the FRF shown in Figure 3.19.

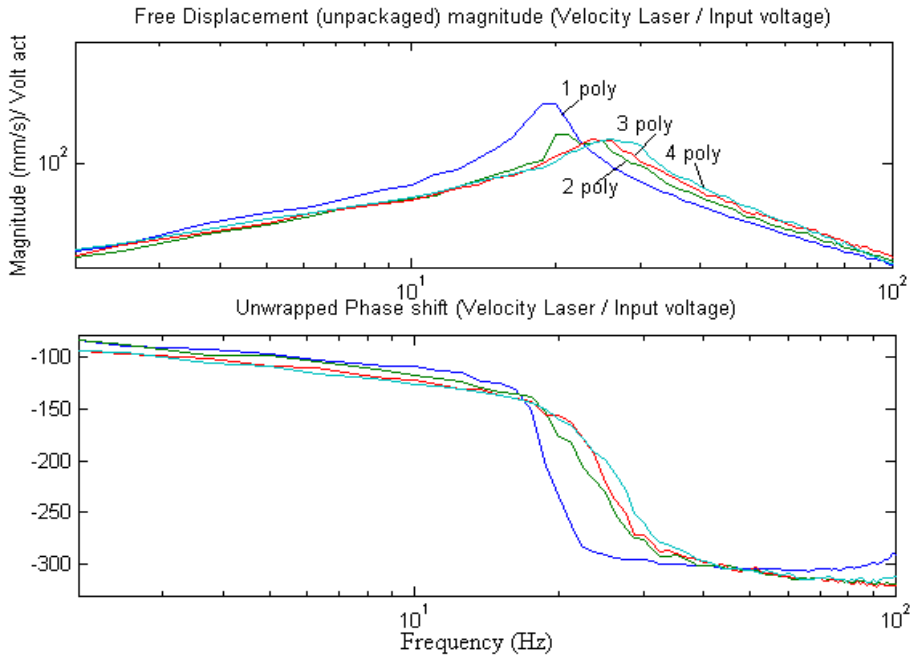

Figure 3.16: Frequency response function for unpackaged stacks parallel stacks

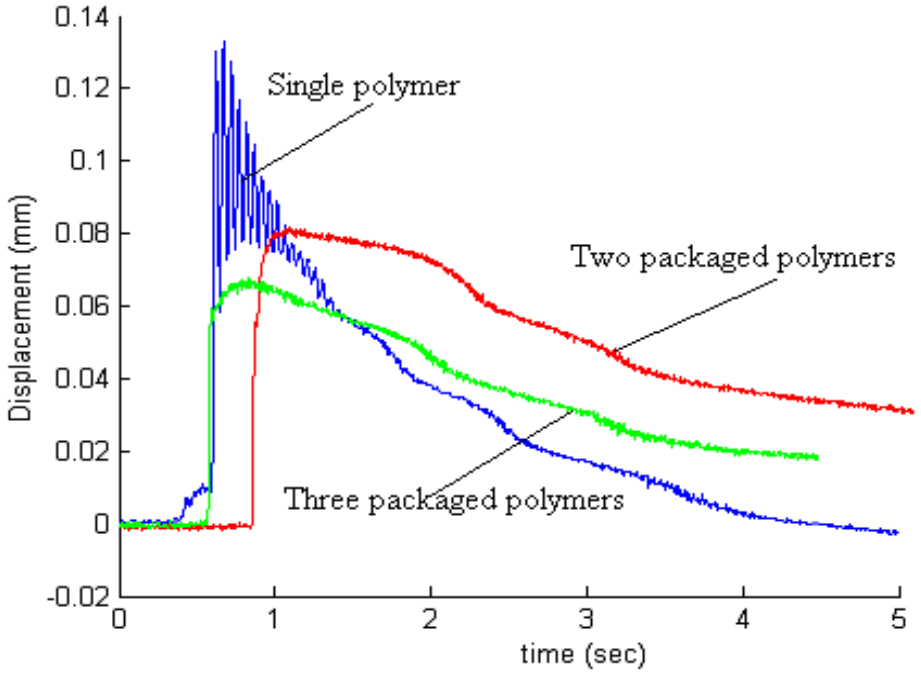

Figure 3.17: Step response for packaged parallel stacks

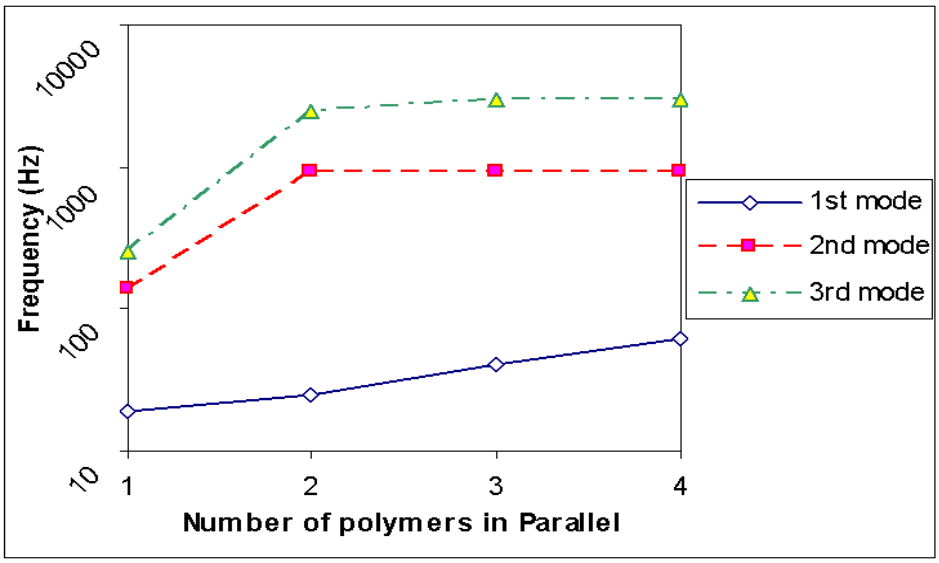

Figure 3.18: Natural frequency variation of packaged stacks

3.5 The Finite Element Analysis method

In this section a Finite Element Analysis (FEA) method is used to numerically simulate the mechanical behavior of ionic polymers. The FEA analysis will be used to explore, verify, and analyze the interfacial friction between layer stacks. FEA is a numerical method that can be used to model and simulate any physical phenomenon of known mathematical model applied to a system. Though we could have created a more complicated multi-physics (electro-mechanical) model, in our case the structural analysis was sufficient. In chapter 5 Newbury's model will be modified and presented, this model is capable of modeling the electromechancial coupling for beam geometries. All the FEA analysis was done using the structural toolbox of ANSYS 6.0 software package. The PLANE82 2 Dimensional 8-Node Structural Solid element was used when a 2 dimensional analysis is required, which is when analyzing the interfacial friction of stacks. Another element was used for the "2 and a half dimension" analysis was the SHELL93 element It is shell element, that can be used to model thin 3 dimensional objects. As mentioned in the previous section, the polymer actuation could be modeled as an internally generated pressure that is trying to overcome the stiffness of the moment in free displacement case, and generating the tip force, in the

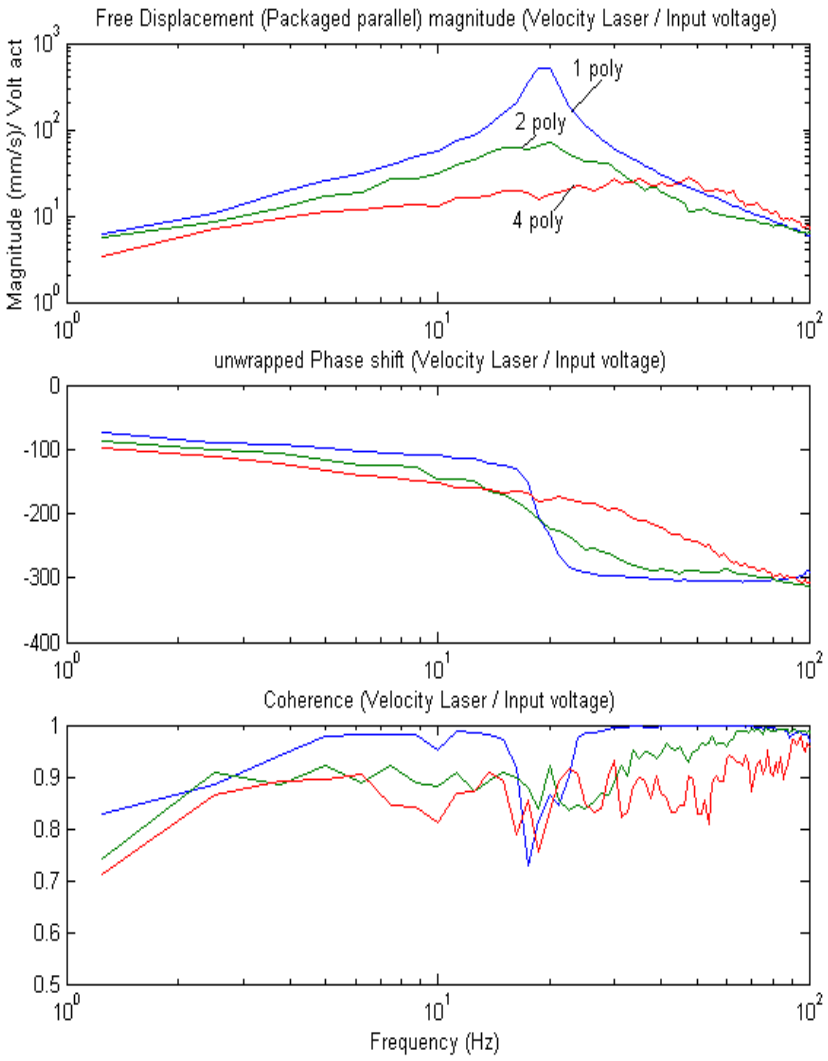

Figure 3.19: The free displacement frequency response for packaged stacks

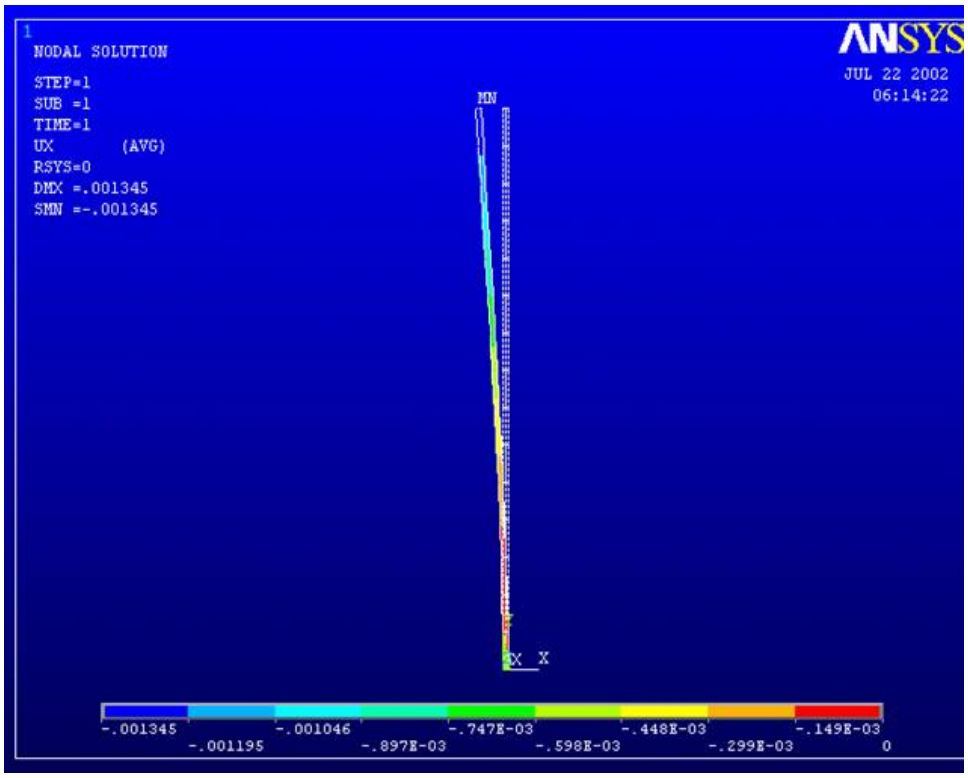

Figure 3.20: The 2D planar model output for the free displacement step input

blocked force case. In the next section we will verify this concept by comparing the experimental results with the numerical data output of the FEA.

3.5.1 Verification of the FEA method

In order to verify this method, we compare the experimental results to the numerical solution. The experimental results are the free displacement, the blocked force, and the natural frequencies. We also measure the mechanical properties of the ionic transducer. The density used is $3100 kg/m^3$, the Poisson's ratio is assumed to be 0.45, and the overall ionic polymer elasticity is computed to be E = 260Mpa. As for the dimensions, we match the data with simulation for the 22mm * 5mm * 0.5mm polymers. In order to verify the experimental model, we use the 2 dimensional planar analyzes shown in Figure 3.20.

The idea was to find the pressure that bends the polymer such that the tip free displacement would match the experimental result of 1.35 mm under applying

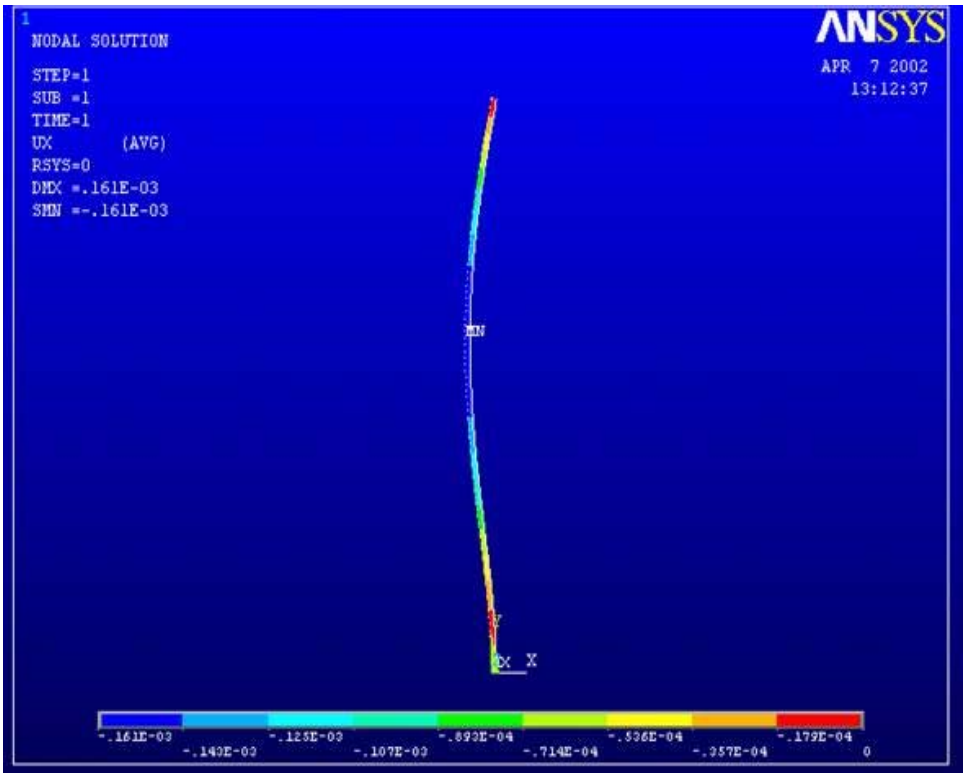

Figure 3.21: The 2D planar model output for the blocked force step input

1.1V across its thickness. The pressure was found to be around 8.5 Pa. Later a model as the one shown in Figure 3.21 was analyzed with the tip blocked, and a pressure of 8.5 Pa applied on it. The reaction on the tip was 0.33 mN, which is within 6% compared to the 0.35 mN experimental result.

The next step is verifying the shell93 element model. A model of identical dimensions and material properties is created using the shell element as shown in figure 3.22. The analysis is done to give 1.353 mm free displacement, and a blocked force of 0.346 mN. In this section the FEA method is verified.

3.5.2 FEA simulations for the parallel stacks

In this section an FEA simulation of the multilayer ionic transducers will be discussed. Also the interfacial friction in the stacks will be simulated and numerical results to experimental will be compared. To simulate the extreme cases of no friction, and no slip, the following assumption was made: For the no slip case (or high friction),

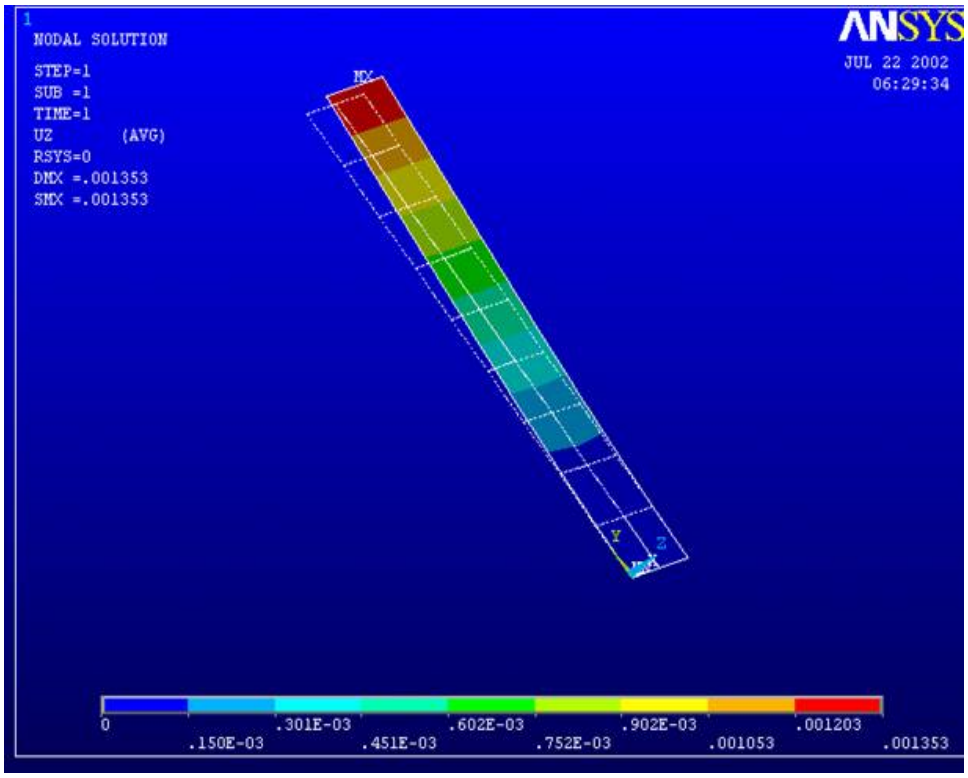

Figure 3.22: The 2D planar model output for the blocked force step input

we can choose from two methods, the first was to "Glue" the polymers together and apply pressure on each polymer. "Glue" is a built in command in ANSYS, that won't allow motion upon the glued nodes. A second method, is to increase the thickness of the polymers such that it is equal to the stack thickness, and apply the overall pressure (n*8.5Pa) on the stack. This method is easier compared to the first method which is more physically representative. Both methods gave the same results gave the same results. As for the no friction model, up till now we were only able to simulate it for the 2D models, in which we can only represent uniformed rectangular stacks. The barrier in upgrading it to the 3D models, was the contact elements, in which ANSYS 6.0 only support linear contact elements, which can not be applied to areas (Areas represent the contact between the layers in a 3D model, while a line represent it in a 2D model). The model consists of drawing the profile of the 2D polymers, apply contact elements on the lines where the layers intersect, and apply the 8.5Pa pressure on each layer.

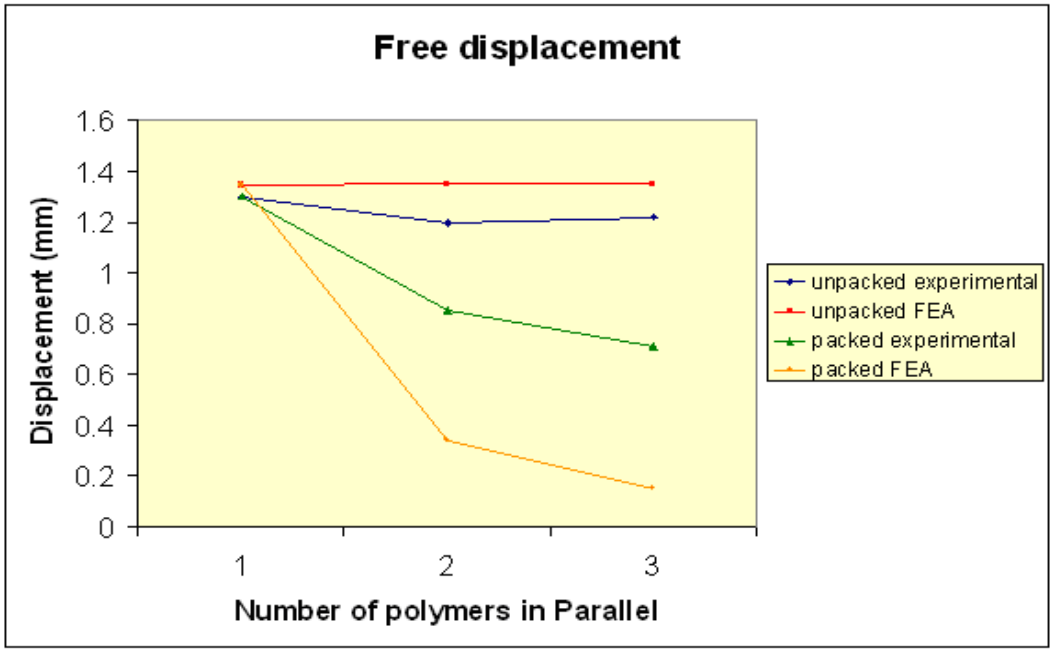

Figure 3.23: The experimental and FEA outputs for packaged and unpackaged free displacement step output as a function of number of polymers.

3.5.3 Analysis of the interfacial friction

As mentioned before, the no friction case could only be modeled using the 2D plane 82 element model. Moreover the stacks could be in 2D, since they are uniform and rectangular. The two extreme cases of no friction and no slip were simulated using the 2D approach for 2 and 3 layers. The results for the free displacement FEA output and the experimental results are shown in Figure 3.23. It can be noticed that the experimental results are included within the extreme cases as simulated with the FEA method.

As previously mentioned the ideal no slip and no friction cases can never be reached, thus as expected the experimental data was within the bounds of the numerical analysis. As for the blocked force, the numerical data also enveloped the experimental data as it can be seen in Figure 3.24.

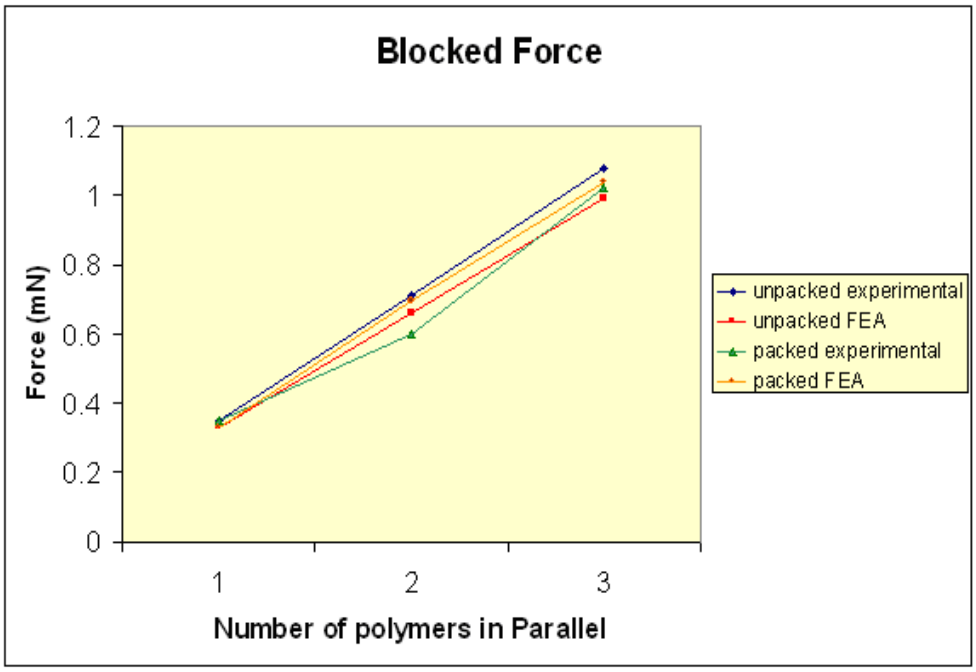

Figure 3.24: The experimental and FEA outputs for packaged and unpackaged blocked force step output as a function of number of polymers.

3.6 Summary

In this chapter the stacking process was thoroughly explained and characterized. First the series and parallel stacking techniques were introduced and compared. Also emphasized was the simplicity and reliable use of series stacking versus the better performance of the parallel stacking. After the manufacturing process, the stacks were characterized as actuators and sensors. As actuators the force is amplified proportional to the number of layers at a constant voltage for the parallel stacks. The sensor sensitivity also increases proportional to the number of stacks for the parallel multilayer stacks. As for series, the saturation voltage will increase proportional to the number of layers, while the force will remain constant if the stack voltage was not increased. As sensors, series stacking improve the sensitivity of the transducer. Further characterization conclusions were made concerning the free displacement, and the resonance frequency, in parallel with the interfacial friction between the stack layers. It was shown that if the interfacial friction was zero, the stack will act as a single layer, by conserving its large free displacement, and low resonance frequencies.

While in case the friction was so high that the polymers couldn't move with respect to each other, the free displacement will decrease proportional to $\frac{1}{N_L^2}$, while the natural frequency will increase. Finally an FEA method was explained, verified, and used to numerically validate the previous conclusions. In the FEA method two types of analysis was explored, one using the planar 2D approach, which is suitable to simulate all types of problems that could be simulated in 2D (e.g. rectangular stacks.) The second was the shell 3D method, which could be used to simulate any polymer sheet shape, with the drawback of being able to simulate extreme interfacial friction cases only.

Chapter 4

Combined Sensor-Actuator Stacks

4.1 Introduction

The primary purpose of this chapter is to describe and characterize the combined sensor-actuator stack. As mentioned in the introduction, ionic polymers show hysteresis during operation and relax after a step input. Researchers proved that those problems could be solved using feedback control. Furthermore feedback control adds robustness to the operation of a system. These results lead us to the development of the combined sensor-actuator stacks which have the actuator and the feedback sensor embedded in it. In the beginning of the chapter, the combined sensor actuator is compared to the self-sensing piezo actuator (sensuator). Next the fabrication technique with all its difficulties will be explained, and a special focus about the electrical connections and insulation will be provided. The feed-through issue is explored in depth in the last section. The problem is characterized and different sources are discussed.

4.2 Combined Sensor vs. Self-sensing Actuator

The self-sensing actuator by definition is the simultaneous sensor/actuator. In piezoelectric stacks the sensuator was initially developed by Dosch, Inman, and Garcia. Self-sensing actuator is the use of the same piezo stack used as an actuator and feedback sensor. The concept of a sensuator works due to the electromechanical coupling

Material Property	Ionic Polymers	Piezo PSI-5A 4E Ceramic
Piezoelectric Strain Coefficient d_{33} (m/V)	1.5×10^{-8}	3.9×10^{-10}
Dielectric Permitivity η_{33}^T (F/m)	1×10^{-2}	1.6×10^{-8}
Elastic Compliance s_{33}^E (m^2/N)	3.3×10^{-9}	1.5×10^{-11}
k_{33}^2 ($N m/V^2 F$)	6.8×10^{-6}	6.3×10^{-1}

Table 4.1: Material property comparison between ionic polymers and piezo PSI-5A 4E ceramic (Newbury (2002) and Piezo Systems (2003))

of piezoelectric material. For the sensuator to be effective, the sensing signal should be in the same order of magnitude or larger than the actuation signal. The following is the charge equation in case a voltage is applied across the stack:

$$\frac{q(s)}{V(s)} = \frac{n\eta_{33}A}{t}\left[\frac{k_{33}^2 k_p}{m s^2 + cs + k + k_p} + (1 - k_{33}^2)\right] \tag{4.1}$$

The term $\frac{n\eta_{33}A}{t}$ is the stress free capacitance, $\frac{k_{33}^2 k_p}{m s^2 + cs + k + k_p}$ is the charge induced due to mechanical motion, and $(1 - k_{33}^2)$ is the charge due to the electrical exitation (Leo course notes, 2001). Therefore the critical term for the sensuator is the $k_{33}^2 = \frac{d_{33}^2}{\eta_{33}^T s_{33}^E}$, which is desired to be as large as possible (so that the term $(1 - k_{33}^2)$ is as small as possible). The term d_{33}^2 is the square of the piezoelectric charge constant, s_{33}^E is the short circuit mechanical compliance, while η_{33}^T is the stress free capacitance of the material.

Considering table 4.1 shows that the k_{33}^2 coefficient for the piezoelectric material is 5 orders of magnitude larger than the coefficient for ionic polymers. Although the piezoelectric strain coefficient is two orders of magnitude larger for ionic polymers as compared to piezoceramics, the electric and mechanical impedances are much larger in ionic polymers than it is in piezoelectric materials. The permittivity of ionic polymers is six order larger than piezoceramics, and the compliance is two orders larger. Therefore the overall value of k_{33}^2 is very low in ionic polymers, such that experimentally there is no sensible change between blocked and free boundary conditions (Newbury, 2002). A conclusion would be that the sensuator concept is practically impossible for the current ionic polymer materials; this is another reason that led us to the development of the combined stacks.

4.3 Alternative configurations

With the increase in the need of accurate devices, feedback control became a necessity in all type of actuators. Therefore feedback is required for the proper use of ionic polymers as actuators. Several researchers, including Curt Cothera in CIMSS Lab worked on using the laser vibrometer as a feedback sensor (Kothera, 2002). Newbury developed a rotating motor that is actuated by four ionic polymers and the feedback was done via a fifth ionic polymer This device was designed for the purpose of verifying the model he proposed for Ionic polymers. The major difference between our works is the compactness. Newbury's device is much larger than a stack for the same power and properties. But the major drawback of the combined stack is the feed-through problem which will be explained and characterized thoroughly in a later section.

4.4 Fabrication

Combined stacks can be manufactured in different configurations. The configuration used in most of this analysis is the one sensor and two actuators connected in parallel stack. This configuration can be justified depending on the application. For example if high forces are required more actuating polymers will be added, while if more accuracy is required, more sensors in parallel will be added. One aspect of the design is the mechanical behavior of the overall stack. The same analysis made in Chapter 2 for the interfacial friction and the FEA methods still apply with minor changes which will be described in the next section. Before going into the analysis of the combined stacks, we will first explore the way in which we made the electrical connections.

4.4.1 Electrical connections

Each stack is manufactured separately as described in the previous sections of parallel stack manufacturing. For both the sensors and the actuators we are only interested in parallel connections for the to combined stacks. Series stacking can never be an advantage for packaged actuator stacks because series stacks require higher voltages to

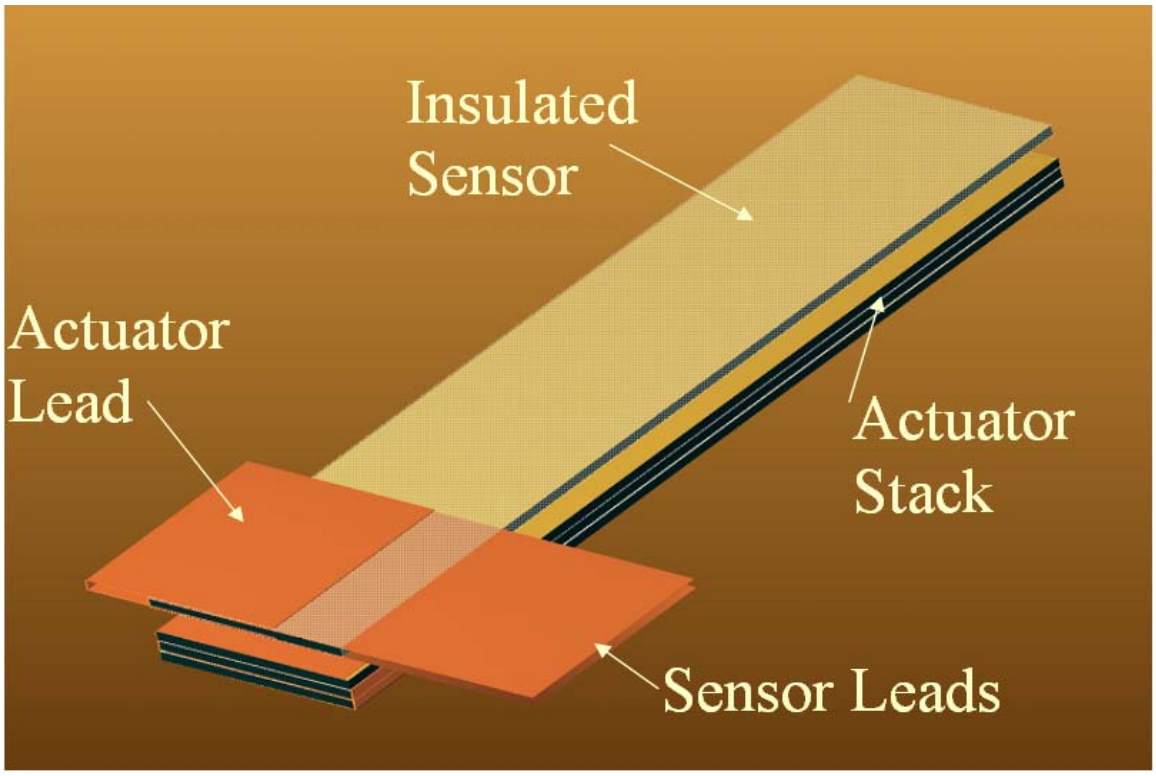

Figure 4.1: A 3D CAD drawing representing the combined stack.

operate. Higher voltages induce electrolysis and result in the drying of the polymers. With regards to the sensing mechanism, as long as we are using the current amplifier circuit it is not advantageous to stack the polymers in series. (Refer to chapter 3 for further information on this subject). After building the sensor stack and the actuator stack, the electric connections are supplied independently to the two stacks. In our case we only needed to supply connections to the sensor, since the actuator stack has been supplied from the leads on the test fixture support base.

Each stack is then separately insulated and layered on top of each other mechanically as shown in Figure 4.1. In this figure is shown the configuration we fabricated for the experimental analysis, where the power to the actuator stack is provided via the support leads.

Another important issue used to improve the performance is the use of a common ground for the sensor and actuator elements. This is accomplished by connecting the sides facing each other between the sensor stack and actuator stack as shown in

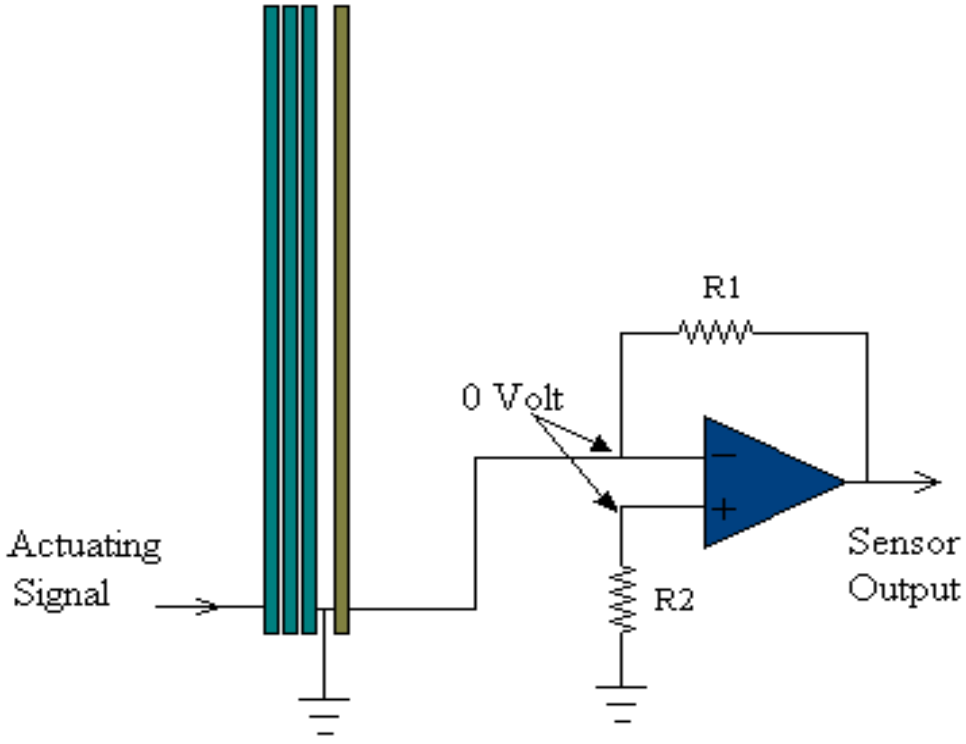

Figure 4.2: Schematic drawing showing the electric connections of the combined stack

the schematic in Figure 4.2. This is important because we are using a current amplifier for the sensor, and the current amplifier forces the sensor to be ground (the current amplifier is also known as short circuit measuring technique). Thus if the sensor is forced to zero, while on the other side across the insulation, there is a high applied voltage (in order to actuate the stack a small current will be induced. This current will disturb the feedback signal, and contribute to the noise, which is the feed-through signals. Although we are using insulating materials which makes this resistance very high, but this material is very thin in order for it to preserve the large displacement. Furthermore the current generated by the sensor is very small, in the order µAmps, thus any noise in the current signal will be significant and could result in a loss of sensing capability

4.4.2 Mechanical properties and the FEA method

According to Newbury (2002), ionic polymers doesn't change there mechanical or electrical impedances as a function of boundary conditions. Therefore from the mechanical structural perspective there is no difference between a sensor or an actuator. Thus combined stacks are treated mechanically as series and parallel transducers, with two slight differences. The first difference is the fact that not all polymers are actuators, therefore the large displacement of the single actuator can never be conserved in the combined stack because the sensor's stiffness will act as an extra load on the actuators. Moreover it is very difficult to achieve the zero interfacial friction case because the stacks have to be packaged.

As for the FEA method, the only change in the analysis would occur in applying the pressure force on the actuator polymers only. Furthermore it is best to model the stacks as zero slip between the layers.

4.5 Characterization of the combined stacks

Combined stacks are characterized experimentally by applying a potential across the actuator stack similar to series or parallel multilayer stacks. While the sensor is connected to the current amplifier using its own electrodes. For characterization purposes the actuator stack is sometimes turned off and an external mechanical deformation is applied using the shaker. This is done in order to obtain the FRF of the sensor without any possibility of having feed-through.

Figure 4.3 shows a comparison for a sensor characterized using the two methods. It is evident that there is some difference in the response, especially in the low frequency range. This could be associated with the way the polymer is mechanically actuated in the different combinations. In the shaker the polymer is actuated on the tip while in the combined stack the actuating polymer is applying the force. The difference the applied loads for the two cases could account for the differences in the measured sensing response.

The combined stacks are to be used in feedback control, thus in this section the

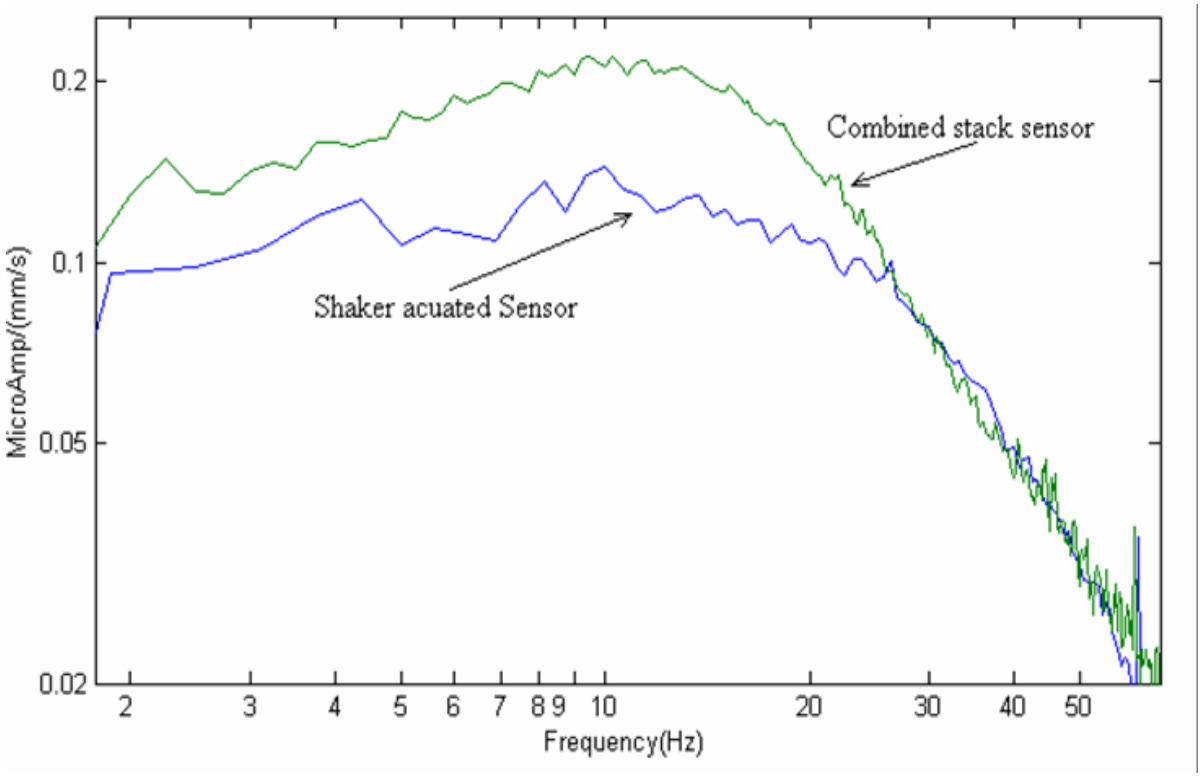

Figure 4.3: Two FRF function for the same stack, one sensed with a polymer sensor and the other with laser vibrometer.

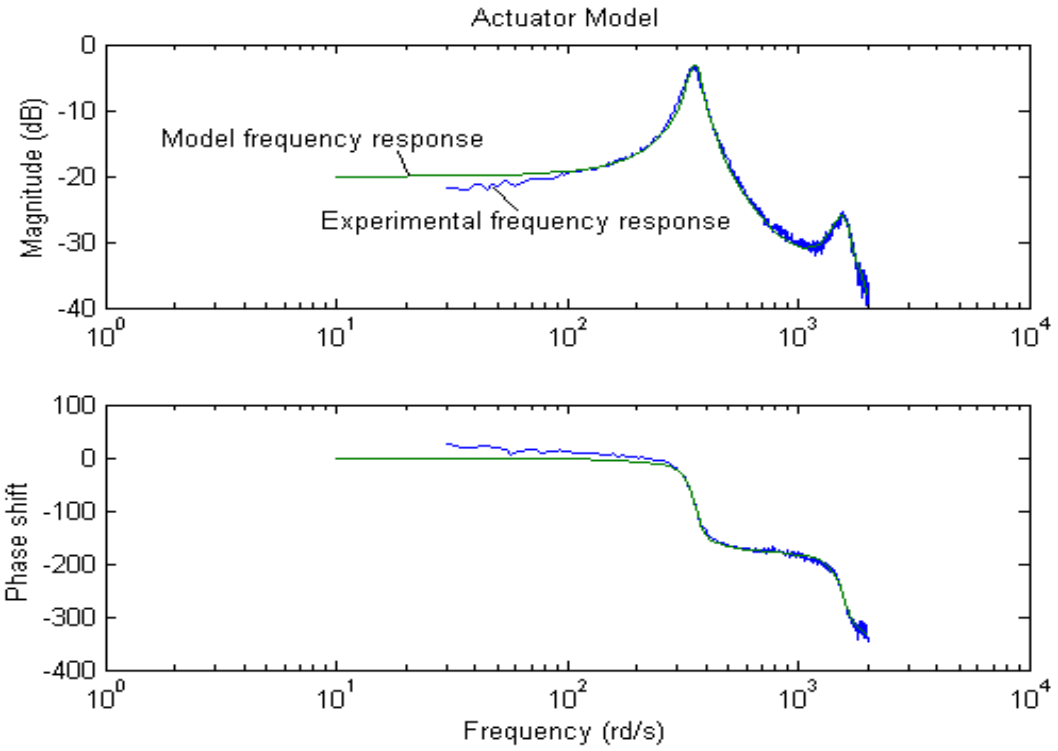

Figure 4.4: The experimental and model transfer functions of the actuator.

experimental FRFs (or transfer functions) of the combined stacks will be displayed and fitted with a Laplace domain model.

Also the Laplace domain transfer function was computed using the "invfreqs" Matlab command, for both the sensor and the actuator. The transfer function for the actuator is

$$G(s) = \frac{0.001589s^4 + 0.07389s^3 - 1.964 \cdot 10^5 s^2 + 7.753 \cdot 10^8 s + 4.946 \cdot 10^{13}}{s^4 + 2205s^3 + 1.032 \cdot 10^8 s^2 + 4.313 \cdot 10^{10} s + 4.96 \cdot 10^{14}},$$

and the frequency response plot with the experimental data is shown in Figure 4.4.

As for the sensor, the Laplace domain transfer function is

$$H(s) = \frac{-0.53s^3 - 327.4s^2 - 3.054 \cdot 10^5 s + 2.817 \cdot 10^6}{s^4 + 571.8s^3 + 2.346 \cdot 10^5 s^2 + 2.238 \cdot 10^7 s - 2.238 \cdot 10^5},$$

and the frequency response plot is shown in Figure 4.5.

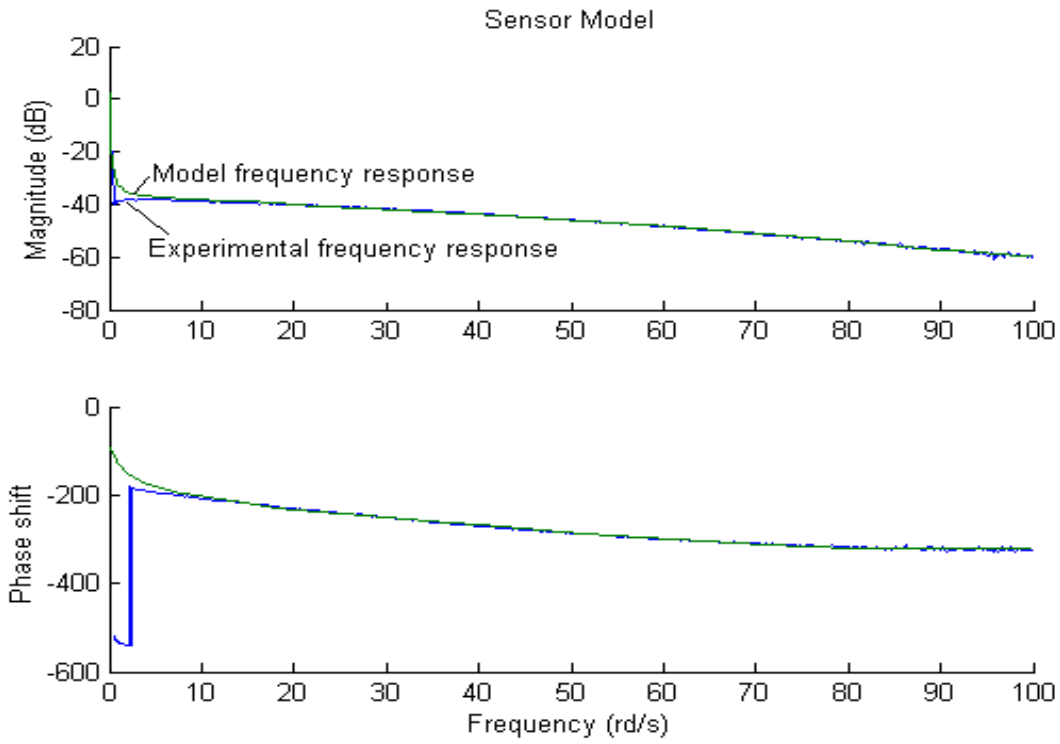

Figure 4.5: The experimental and model transfer functions of the sensor.

4.6 Feed-through

Feed-through is defined as the part of the sensed signal (feedback) directly transmitted from the input signal. If large enough, the feed-through signal will dominate the feedback signal; it could be as hundreds if not thousand times the feedback signal and it will immediately saturate the amplifier circuit.

A comparison between a clean signal and a signal with feed through is shown in Figure 4.6. It has different sources, which can be put in three main categories. The most important is the direct feed-through the water, or water vapor existing between the sensor, and the actuator stacks, the second is the feed-through the insulation film between the sensor and actuator stacks. Those mentioned feed-through are both resistive in nature, while the third type is magnetic, which is due to the current flowing in the actuating polymer circuitry. Magnetic feed-through is insignificant; therefore we believe that water transport is the primary cause of feedthrough.

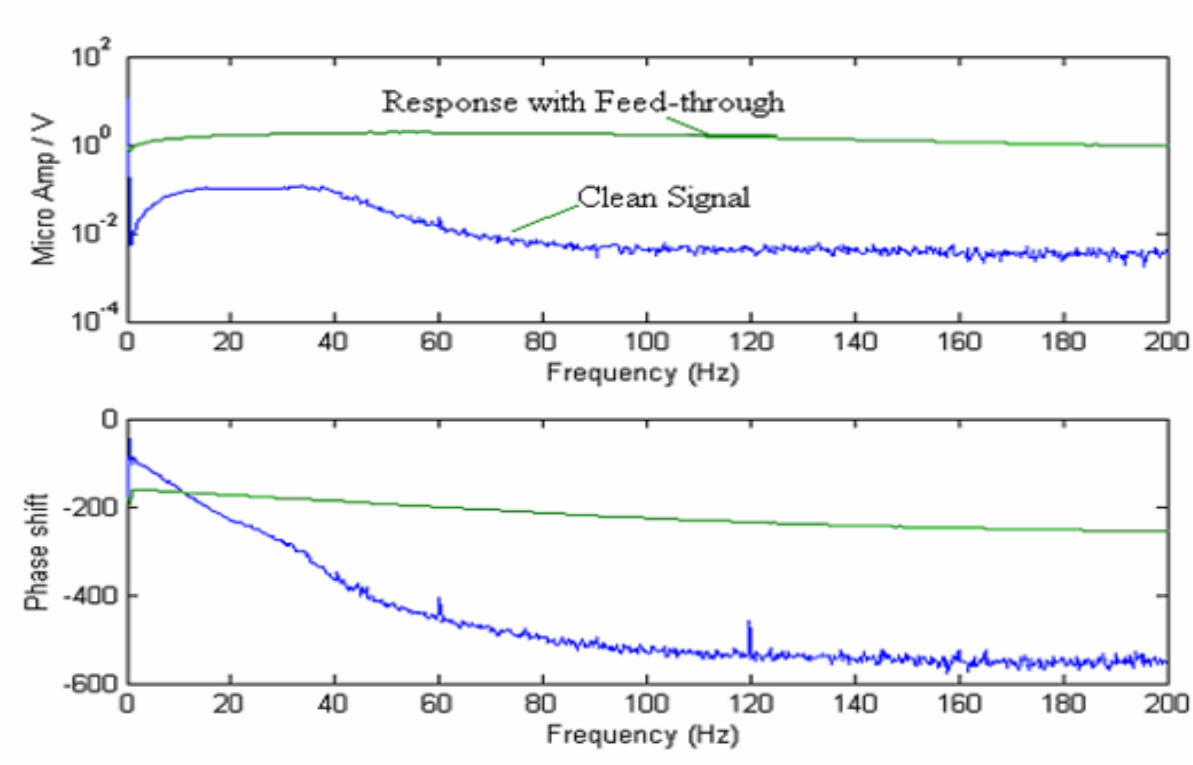

Figure 4.6: The FRF of different combined stacks, one with feed through and the other without.

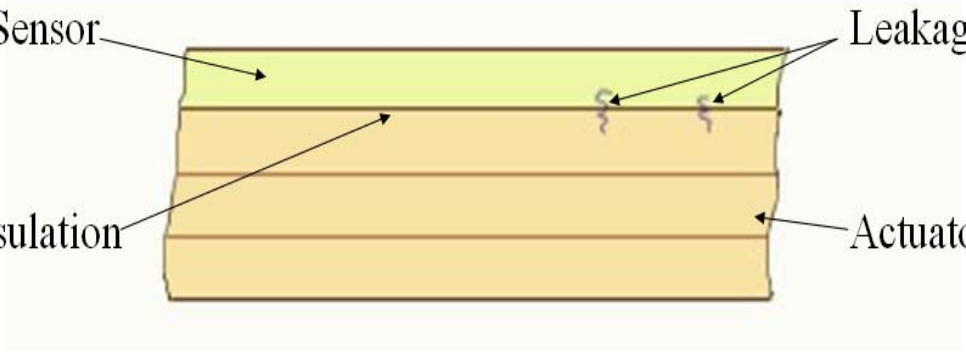

Figure 4.7: Schematic drawing showing the feed through between the sensor and the actuator

4.6.1 Insulation

The main two sources of feed-through are the water and the insulation film between the stacks. To start with the easy problem of the insulation film, as mentioned in section 1.4.1, most of this problem was solved by forcing the actuator layer facing the sensor stack to ground, and applying the positive and negative voltages on the side. This technique was able to solve most of the problem, and made this feed-through insignificant. Nonetheless some small voltages will still appear on the tip of the polymer, since the ground is applied on the base of the polymer, and the polymer surface has a finite value resistance. Thus once can still find some positive or negative small voltages on the tip. But again those voltages are very small, and the resistance value of the insulation is very large, therefore we don't have to worry about this very much.

The second source of feed-through is the water between the stacks as shown in Figure 4.7 . As previously mentioned it is the main source of feed-through, and the most difficult to deal with. For proper operation, ionic polymers need to be well hydrated, therefore water should exists all around the stack. Water is a good conductor of electricity, even in the form of moisture. Thus water insulation between the stacks is very essential. Moreover the polymer combined stacks should be designed to sustain higher frequencies, which makes easier for water to flow around the stack, especially at the tip. The pressure build-up at the tip of the stacks was remarkable

during the operation of frequencies in the order of 50Hz and above. To conclude insulation between the two stacks is very essential, especially the insulation against humidity is a very critical issue. As for the electric insulation, it became a minor problem since it was resolved by the use of the common ground technique. In the next section the feed-through will be characterized so that it can be better detected and resolved.

4.6.2 Characterization of feed-through

The main sources of feed-through are the water feed-through, and the insulation resistance feed-through. They are both resistive loads in nature, thus the signal is directly fed through the sensor stack without any delay (phase shift). As mentioned in section 2.3.1 the ionic polymer connected to the current amplifier circuit forms a low pass RC filter. This is why it is expected to see the feed-through as a linear signal imputed to a low pass filter as shown in Figure 4.6 . The feed through signal in Figure 4.6 was obtained by creating a small break in the insulation between the stacks, and computing the FRF.

4.7 Summary

In this chapter the combined stacks were thoroughly explored and characterized. First they were compared to the sensuator concept, and there potential applications were explored. Next the fabrication techniques were explained, and the combined stack was characterized. In the final section an emphasis on the feed-through problem was highlighted. A conclusion of this chapter would be to point the importance of the combined stacks, and their ability to many problems related to ionic polymers. Their major drawback is the feed-through problem which requires extra care during the fabrication process, and need to be given attention if this process is to be automated. As in the conclusion of the previous chapter, the combined stacks fabrication needs to be moved to the micro level in order to be very effective and useful.

Chapter 5

Modeling multilayer stacks

5.1 Introduction

In this chapter the model developed by Newbury and Leo (2002) is extended so that it is able to model multilayer polymer stacks. For design and characterization purposes multilayered ionic polymers are fitted to a mathematical model that is able to predict their performance. As mentioned in Chapter 1, there are several models that could be used for ionic polymers. For completeness and practicality purposes Newbury's empirical model was used. The main advantages of this model are that it is accurate and easy to use and it also considers both the actuation and sensing characteristics of ionic polymers. In the first section, a brief overview of the model is presented. In the second section, the mathematical model is modified to fit the multilayer stacks. While the third section, the experimental results are used to obtain the model parameters. Finally a chapter summary is provided.

5.2 Model Overview

Newbury's model is developed to be used in modeling single layer ionic polymers with cantilever boundary condition. Being a scalable to the polymer geometry, this model was made easy to be adjusted to simulate the multilayer stacks. In this model

ionic polymers are presented with an equivalent ideal transformer circuit model. It also assumes that the electrical and mechanical domains are linearly coupled. Thus the constitutive relations consist of two linearly independent symmetric equations,

$$\begin{bmatrix} v \\ f \end{bmatrix} = \begin{bmatrix} a_{11} & a_{12} \\ a_{12} & a_{22} \end{bmatrix} \begin{bmatrix} i \\ u \end{bmatrix} \tag{5.1}$$

Where v is the voltage across the polymer thickness and f is the force at the tip. As for i is the current across the polymer's thickness, and u is the velocity at the tip. The coefficients a_{11}, a_{12}, and a_{22} are functions of the material parameters and bender geometry. Before explaining those parameters, it is important to note that equation 5.1 is similar to the piezoelectric constitutive equations, therefore a similar approach is adopted to determine the coefficients. This approach consists of setting some parameters to zero in compute the remaining parameters. Obtaining the model parameters will be explained in a later section, but setting one parameter to zero and considering the equation enables us to easily identify the coefficient. To start with a_{11} coefficient, setting $u = 0$ reduces the upper part of equation 5.1 to

$$v = a_{11} i, \tag{5.2}$$

which reduces a_{11} to the electrical impedance of the material. Similarly, setting $i = 0$ reduces the lower part of equation 5.1 to

$$f = a_{22} u. \tag{5.3}$$

The term a_{12} is the electro-mechanical coupling term which relates the displacement to the actuation voltage, and the current generated due to the applied mechanical force or stress. Now reconsidering the ideal transformer equivalent circuit model shown in Figure ?? and using any basic circuit analysis technique will result in the following results for the coefficients used in equation 5.1,

$$\begin{bmatrix} v \\ f \end{bmatrix} = \begin{bmatrix} \frac{R_{dc}(N^2 Z_{m1} + Z_p)}{R_{dc} + N^2 Z_{m1} + Z_p} & \frac{N R_{dc} Z_{m1}}{R_{dc} + N^2 Z_{m1} + Z_p} \\ \frac{N R_{dc} Z_{m1}}{R_{dc} + N^2 Z_{m1} + Z_p} & \frac{(Z_{m1} + Z_{m2})(R_{dc} + Z_p) + N^2 Z_{m1} Z_{m2}}{R_{dc} + N^2 Z_{m1} + Z_p} \end{bmatrix} \begin{bmatrix} i \\ u \end{bmatrix} \tag{5.4}$$

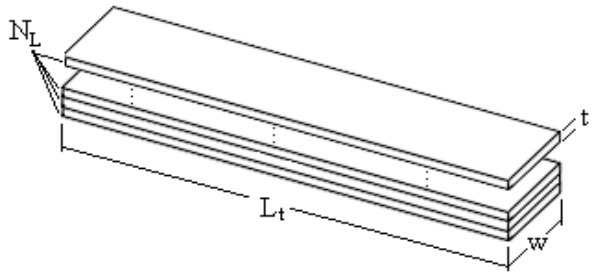

Figure 5.1: The geometric parameters of the stack.

The last step in the model development is determining the electromechanical terms in equation 5.4, which are the same variables in Figure ??. This is discussed in the next section with the modification implemented to incorporate the multilayer ionic polymers.

5.3 Describing and Modifying the Electromechanical Terms for Multilayer Stacks

The following terms are to be developed and modified to extend the model to multilayer stacks: the mechanical terms Z_{m1} and Z_{m2}, the electrical terms R_{dc} and Z_p, and the electromechanical coupling term N. The modification will be established for the different stacking cases. The first variable would be the type of electrical connections; the options are parallel and series connections. The second variable would be the interfacial boundary condition; the first case would be no slip, while the second would be no friction.

5.3.1 The Electrical Terms

The electrical impedance is described by the two terms, R_{dc} and Z_p. The first term R_{dc} is the DC resistance defined in the following equation

$$R_{dc} = \frac{\rho_{dc} t}{L_t w}, \tag{5.5}$$

where ρ_{dc} is the resistivity of the polymer, while the other parameters are the geometry of the polymer as defined in Figure 5.1. As for modifying this term to account for multilayer stacks, it's good to note that the mechanical boundary condition doesn't have any significant effect on the electrical terms (Newbury, 2002), thus the only variable to be considered would be the type of electrical connections. The term R_{dc} is the DC resistance of the material, and resistors add in series while in parallel it is the inverse of the sum of the inverse. Therfore the resulting equation for R_{dc} in case of N_l (This is defined as N_l to avoid confusion with N the number of turns in the coil) polymers connected in series is

$$R_{dc} = \frac{N_l \rho_{dc} t}{L_t w}. \tag{5.6}$$

In case they are connected in parallel the equation is

$$R_{dc} = \frac{\rho_{dc} t}{N_l L_t w}. \tag{5.7}$$

As for Z_p the equation for single layer polymer is obtained form Newbury's dissertation to be

$$Z_p = \frac{t}{sL_t w} \left[\frac{1}{\sum_{i=1}^{n} \frac{\alpha_i}{1 + s\alpha_i \rho_i}} \right] \tag{5.8}$$

where n, α_i, and ρ_i, are to be determined numerically from experimental data. Since this is another form of electrical impedance the same rules as in R_{dc} case. Therefore the equation for the parallel electrical connections becomes:

$$Z_p = \frac{1}{N_l} \frac{t}{sL_t w} \left[\frac{1}{\sum_{i=1}^{n} \frac{\alpha_i}{1 + s\alpha_i \rho_i}} \right] \tag{5.9}$$

as for series it is :

$$Z_p = N_l \frac{t}{sL_t w} \left[\frac{1}{\sum_{i=1}^{n} \frac{\alpha_i}{1 + s\alpha_i \rho_i}} \right] \tag{5.10}$$

5.3.2 The Mechanical Terms

The mechanical terms consist of Z_{m1} and Z_{m2}, and the stacking parameters that affects those terms are the mechanical boundary conditions that are a function of

the inter-facial friction. As for the electrical connections, theoretically it has no significant effect, but practically due to the addition of non-active insulation layers and the electrical leads added to the parallel stack it would change the mechanical terms. For the single layer polymer, the mechanical stiffness is represented by Z_{m1} is computed using Euler-Bernoulli beam model. According to Newbury (2002) the Laplace domain representation is

$$Z_{m1} = \frac{1}{s} Y w t^3 \frac{}{4L_d^3}, \tag{5.11}$$

where

$$Y = Y_\infty \left[1 + \alpha \frac{s^2 + 2\xi\hat{\omega}}{s^2 + 2\xi\hat{\omega}s + \hat{\omega}^2} \right] \tag{5.12}$$

and α, ξ, and $\hat{\omega}$ are the frequency dependent parameters, computed from the GHM model (Newbury, 2002). On the other hand the equation for Z_{m2} which represents the inertia of the polymer, is computed according to the following

$$Z_{m2} = s \frac{3L_{free}^4 \rho_m w t}{L_d^3 \Gamma^4} \tag{5.13}$$

where ρ_m is the density of the polymer and Γ is the solution of the Euler-Bernoulli Beam characteristic equation. For the first mode in a clamped free boundary condition the value is 1.875. To modify the mechanical terms to incorporate the multilayer stacks, start with the simplest case of series electrical connections with zero slip mechanical boundary conditions. In this case the stack will be treated as a single polymer with a thickness proportional to the number of layers

$$t_{stack} = N_l \cdot t \tag{5.14}$$

. and therefore the mechanical terms will be written as follows:

$$Z_{m1} = \frac{N_l^3}{s} Y w t^3 \frac{}{4L_d^3} \tag{5.15}$$

and

$$Z_{m2} = s N_l \frac{3L_{free}^4 \rho_m w t}{L_d^3 \Gamma^4} \tag{5.16}$$

In case of zero interfacial friction, the polymers will act as springs stacked in parallel, which the overall value is the addition of the single ones. The mechanical terms are described as follows:

$$Z_{m1} = \frac{N_l}{s} \frac{Y w t^3}{4 L_d^3} \tag{5.17}$$

and

$$Z_{m2} = s N_l \frac{3 L_{free}^4 \rho_m w t}{L_d^3 \Gamma^4} \tag{5.18}$$

As for the electrical variables, the problems would be with the parallel stack, where some insulation material is added between the polymers, as discussed in Chapter 2. This insulation is a non-active layer that would increase the stiffness of the stack and could be modeled as the polymers themselves. But for our purpose, those stiffness are relatively small and could be neglected. Another minor problem is the electrical leads which has a finite thickness. But those leads are usually placed in the clamped part of the stack; therefore their effect under such circumstances is to be neglected.

5.3.3 The Electromechanical Term

The term which represents the electromechanical coupling in the model is N, the number of turns of the transformer. The turns ratio N is allowed to be a function of frequency. In the model defined by Newbury:

$$N = \left[\frac{v}{f} \right]_i = \frac{3 d L_d^2}{\eta^T L_t w t} \tag{5.19}$$

In order to obtain the equation for both the multilayer stacks, we have to assume that each single layer polymer has a constant

$$N = N_s = \left[\frac{v_1}{f_1} \right]_i = \left[\frac{v_2}{f_2} \right]_i = \ldots = \left[\frac{v_{N_l}}{f_{N_l}} \right]_i = \text{constant} \tag{5.20}$$

As mentioned before, all the stacks discussed in this thesis are layered mechanically in parallel, leading to a constant velocity accross the layers. In order to simplify the problem N is multiplied by the stiffness $\left\langle \frac{f}{u} \right\rangle$ to transform the force into velocity

$$N \left\langle \frac{f}{u} \right\rangle = \left\langle \frac{v}{f} \right\rangle \left\langle \frac{f}{u} \right\rangle = \left\langle \frac{v}{u} \right\rangle, \tag{5.21}$$

According to Newbury $\left\langle \frac{f}{u} \right\rangle = Z_{m1} + Z_{m2}$, which reduces the number of turns to

$$N = \left\langle \frac{v}{u} \right\rangle \frac{1}{Z_{m1} + Z_{m2}}, \tag{5.22}$$

In order to develope N for all of the four boundary conditions, first we start with the no friction interfacial condition. According to equations 5.17 and 5.18, the term $Z_{m1} + Z_{m2}$ will scale prortional to N_L. Considering the electrical connections, for series the overall voltage of the stack is the addition of the single layers $v_{total} = N_L v$. While in parallel connection the overall voltage of the stack equals the single layer voltage $v_{total} = v$. Substituting back into equation 5.22 we obtain the following:

No friction:

Series:

$$N = \left\langle \frac{v}{u} \right\rangle \frac{1}{Z_{m1} + Z_{m2}} = N_s \tag{5.23}$$

Parallel:

$$N = \left\langle \frac{v}{u} \right\rangle \frac{1}{N_L (Z_{m1} + Z_{m2})} = \frac{N_s}{N_L} \tag{5.24}$$

The no slip boundary condition is treated only for the low frequency case where $Z_{m2} << Z_{m1}$ and to be neglected. In this case the term $Z_{m1} + Z_{m2}$ will scale prortional to N_L^3. As for the electrical boundary condition, the analysis used in the no friction case is still valid. Therefore N will be scaled according to the following:

No Slip:

Series:

$$N = \frac{\frac{v}{u}}{\frac{i}{u}} \frac{1}{N_L^2(Z_{m1} + Z_{m2})} = \frac{N_s}{N_L^2} \tag{5.25}$$

Parallel:

$$N = \frac{\frac{v}{u}}{\frac{i}{u}} \frac{1}{N_L^3(Z_{m1} + Z_{m2})} = \frac{N_s}{N_L^3} \tag{5.26}$$

5.4 Modified Input-Output Relationships for Multilayer Transducers.

Before exploring the results, first the essential governing equations will be developed for the four different boundary conditions. The model used in this comparison is the simplified model, where the terms $N^2 Z_{m1} << Z_p$ for the blocked boundary condition, and the term $N^2 \frac{Z_{m1} Z_{m2}}{Z_{m1} + Z_{m2}} << Z_p$ for the free boundary conditions are neglected.

5.4.1 Impedances

The electrical impedance will be reduced to $\frac{v}{i} = \frac{R_{dc} Z_p}{R_{dc} + Z_p}$, and the modifications compared to the single layers:

Series:

$$\frac{v}{i} = \frac{N_L R_{dc} N_L Z_p}{N_L R_{dc} + N_L Z_p} = N_L \frac{R_{dc} Z_p}{R_{dc} + Z_p} \tag{5.27}$$

Parallel:

$$\frac{v}{i} = \frac{\frac{R_{dc}}{N_L} \frac{Z_p}{N_L}}{\frac{R_{dc}}{N_L} + \frac{Z_p}{N_L}} = \frac{1}{N_L} \frac{R_{dc} Z_p}{R_{dc} + Z_p} \tag{5.28}$$

According to Newbury the open-circuit mechanical impedance is reduced to the following $\frac{f}{u} = Z_{m1} + Z_{m2}$. While the modifications for the no friction and no slip interfacial boundary condition are:

No friction:

$$\frac{f}{u} = N_L Z_{m1} + N_L Z_{m2} = N_L (Z_{m1} + Z_{m2}) \tag{5.29}$$

No Slip:

$$\frac{f}{u} = N_L^3 Z_{m1} + N_L Z_{m2} \approx N_L^3 (Z_{m1} + Z_{m2}) \tag{5.30}$$

This approxiation is made considering low frequency range where $Z_{m2} << Z_{m1}$.

5.4.2 Actuator Equations

The simplified blocked force is defined as $\left.\frac{f}{v}\right|_{u} = \frac{N Z_{m1}}{Z_p}$ and the modifications for the four boundary conditions are:

No friction:

Series:

$$\frac{f}{v} = \frac{N N_L Z_{m1}}{N_L Z_p} = \frac{N Z_{m1}}{Z_p} \tag{5.31}$$

Parallel:

$$\frac{f}{v} = \frac{\frac{N}{N_L} N_L Z_{m1}}{\frac{1}{N_L} Z_p} = N_L \frac{N Z_{m1}}{Z_p} \tag{5.32}$$

No Slip:

Series:

$$\frac{f}{v} = \frac{\frac{N}{N_L^2} N_L^3 Z_{m1}}{N_L Z_p} = \frac{N Z_{m1}}{Z_p} \tag{5.33}$$

Parallel:

$$\frac{f}{v} = \frac{\frac{N}{N_L^3} N_L^3 Z_{m1}}{\frac{1}{N_L} Z_p} = N_L \frac{N Z_{m1}}{Z_p} \tag{5.34}$$

This implies that in series the blocked force will remain constant for the same applied voltage, while in parallel it will scale proportional to the number of layers. The simplified model for the free displacement is $\frac{u}{v} = \frac{-N}{sZ_p}$ and scales with the number of layers N_L as follows:

No friction:

Series:

$$\frac{u}{v} = \frac{-N}{N_L sZ_p} = \frac{1}{N_L}\frac{-N}{sZ_p} \tag{5.35}$$

Parallel:

$$\frac{u}{v} = \frac{\frac{-N}{N_L}}{\frac{1}{N_L}sZ_p} = \frac{-N}{sZ_p} \tag{5.36}$$

No Slip:

Series:

$$\frac{u}{v} = \frac{\frac{-N}{N_L^2}}{N_L sZ_p} = \frac{1}{N_L^3}\frac{-N}{sZ_p} \tag{5.37}$$

Parallel:

$$\frac{u}{v} = \frac{\frac{-N}{N_L^3}N_L^3 Z_{m1}}{\frac{1}{N_L}sZ_p} = \frac{1}{N_L^2}\frac{-N}{sZ_p} \tag{5.38}$$

Those equations shows how the no slip boundary condition can reduce the large deflection of the polymer, while the no friction and parallel electrical connection was able to preserve large deflections.

5.4.3 Sensor Equations

In Newbury's model the sensor equations are simplified to $\frac{i}{v} = \frac{-NZ_{m1}}{Z_p}$ which is equal to the blocked force $-\frac{f}{v}$ but opposite sign. This concept is the reciprocity presented by Newbury, and it still holds in multilayered ionic transducers. The sensitivity $\frac{i}{v}$ behaves the same as the blocked force if one follows the same analysis in subsection 5.4.2, thus it increases proportional to the number of layers with parallel stacking, while remain constant for series stacking. All those equations are compared to some experimental results in the next section, and agreement could be noticed.

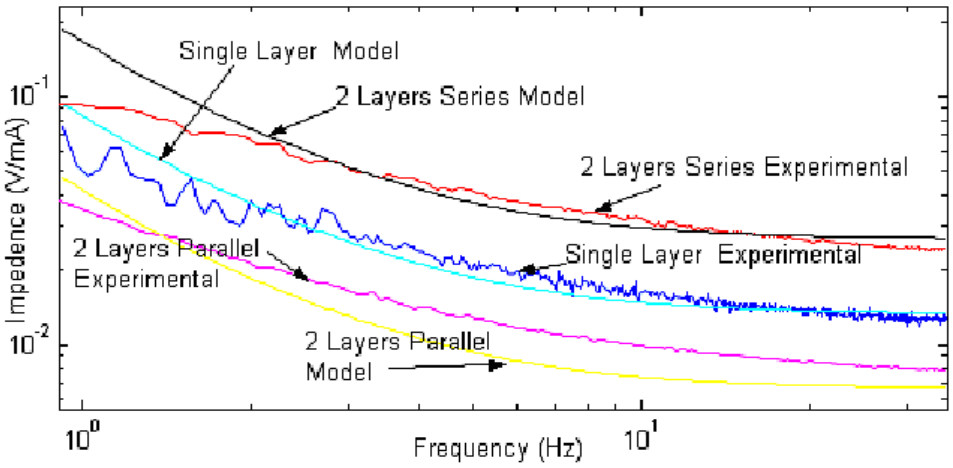

Figure 5.2: Electrical impedance model prediction versus experimental data

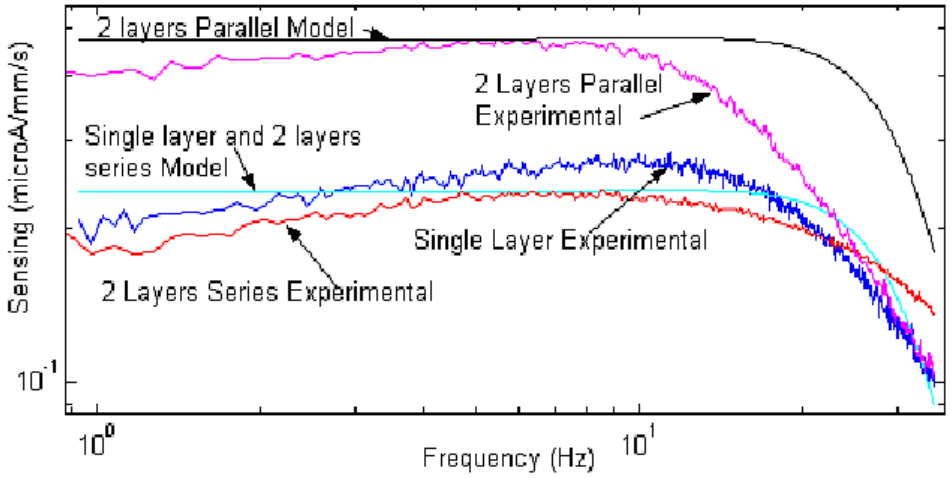

Figure 5.3: Sensitivity model prediction versus experimental data

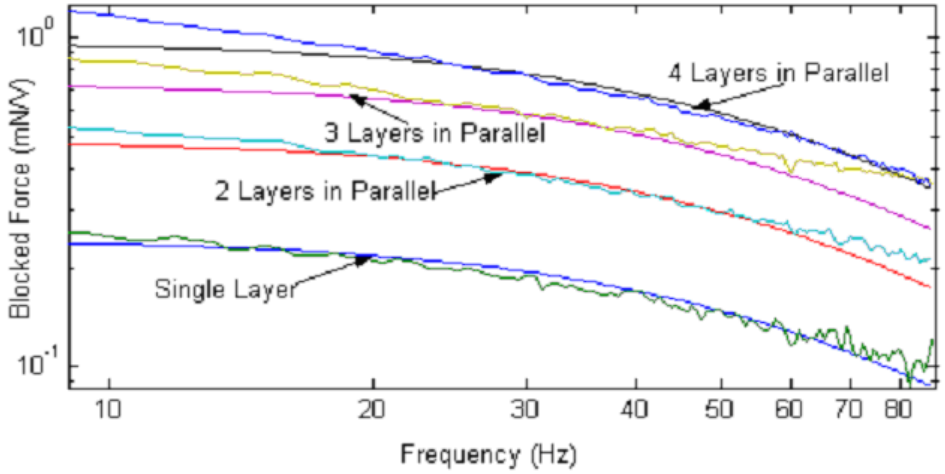

Figure 5.4: Blocked force model prediction versus experimental data

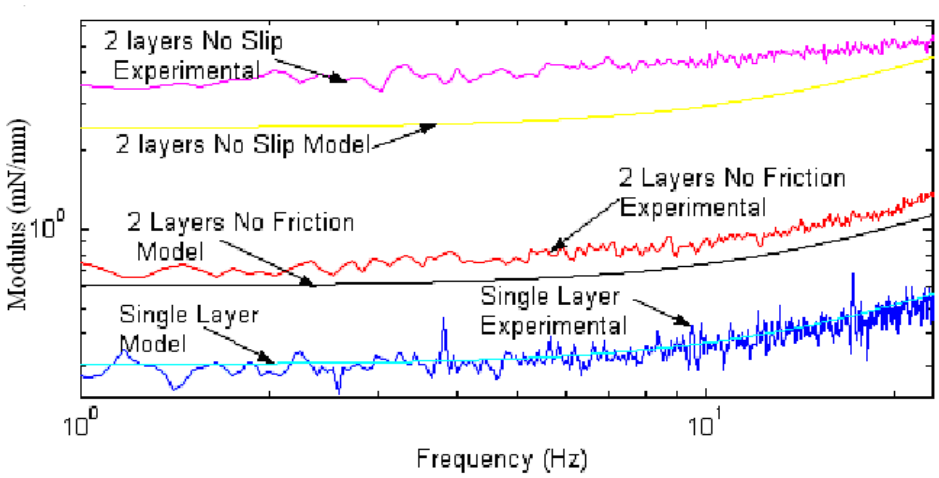

Figure 5.5: Mechanical impedance model prediction versus experimental data

5.5 Comparison of Model with Experimental Results

The model was compared and validated with experimental results. The four terms are the impedance, the modulus, the electromechanical coupling term as sensor, and the electromechanical term as an actuator. The four transfer functions are shown with comparison to the model fitting in Figures 5.2, 5.3, 5.4, and 5.5. For the impedance, the single layer is compared to a 2 layer stack in series, where the model scaled by being multiplied by 2, and it is noticed that the model scaled accurately (see Figure 5.2). On the other hand it was compared to a 2 layer parallel stack, and the model was scaled by 1/2. As it could be noticed from Figure 5.2, this time the model didn't scale accurately (it was 18% o□), and the error is attributed to the resistance in the electric connections. As for the sensing the model fairly scaled the data, which was again compared to a 2 layer series stack, and a 2 layer parallel stack as shown in Figure 5.3. The data for the series configuration is supposed to overlap the single layer but was slightly o□, especially at high frequencies. This is due to the low-pass filter e□ect associated with the current sensing circuit. This assumption is further validated when looking at the parallel stack, which exhibits faster rollover due to the increase in capacitance. The blocked force was compared to 2, 3, and 4

layers parallel stacks, and the model very accurately predicted the increase in blocked force as a function of the number of layers as it could be seen in Figure 5.4. Finally the modulus single layer polymer was compared to 2 layers with different mechanical boundary conditions and shown in Figure 5.5. The first boundary condition of no friction, which is supposed to scale by a factor of 2, was acceptably accurate. While the no slip boundary condition, which is supposed to scale by a factor of $2^3 = 8$, didn't fit well. This might be due to the additional stiffness of the double tape added to achieve the boundary condition of now slip.

5.6 Summary

In this chapter Newbury's model was modified to accomodate the multilayer ionic transducers. First the two port equivalent transformer circuit model was briefly introduced. Than the model was modified on four different boundary conditions, two electrical series and parallel connections, and two mechanical no friction and no slip interfacial boundary condition. The parallel and series electrical connection affected the two electrical impedance terms: R_{DC} and Z_P, and the coupling term N. R_{DC} and Z_P both increased proportional to the number of layers in series connection, and decreased inversely proportional to the number of layers in parallel connection. The electromechanical term is modified by all the four boundary condition. The no friction and series N remained equal to that of a single layer, while the no friction and parallel N is divided by the number of layers. The no slip boundary condition was treated for the low frequency range, and scaled N by dividing it by the square of the number of layers for the series connection, and the the cube of the number of layers for the parallel connection. In the next section the input output relationships for the multilayer transducers were presented. The scaling in the model matched the analysis provided in Chapter 3 from the experimental results. The blocked force and the sensitivity increased proportional to the number of layers in parallel connection, while remained constant for series. The no friction boundary condition also proved to preserve the large deflection, while the no slip boundary condition decreased the

free displacement by the cube of the number of layers for series and the square for parallel. In the last section the model was compared to experimental results. In the low frequency range the matching was very good but it deteriorated at higher frequencies for the sensing test due to the change in capacitance of the transducer.

Chapter 6

Micro Air Vehicle

6.1 Introduction

Finite element simulations on the packaged and unpackaged stacks illustrate that we can accurately model the mechanical response of the transducers. This chapter deals with the design of a flapping mechanism using ionic polymer materials. Ionic polymers are designed to operate and fly a Micro Air Vehicle (MAV). In the next section we are going to propose two wing designs. Those designs are simulated using the previously illustrated FEA method. In the next subsection the mechanical requirements that the ionic polymer has to meet in order to fly the MAV, which are obtained from Wei Shyy et al. (1999) are illustrated. Finally a summary of this short chapter is provided.

6.2 Application: MAV

Micro Air Vehicles (MAV) has several applications in the area of military and civilian autonomous surveillance. In military applications it could be used for short range spying or ammunition guiding functions. Due to its small size, it could be easily camouflaged and hidden from the enemy. Ionic transducers help in this aspect because they tend to be more natural looking. Ionic polymers flap as birds and do not require any mechanical gearing, thus they are also quiet during operation. In civilian

applications MAVs could be used in traffic surveillance.

6.2.1 Design Parameters

Although no aerodynamic modeling was performed on the flapping mechanisms, preliminary numbers were obtained from the review paper by Wei Shyy et al. (1999). The following were used in our study:

- Vehicle weight less than 50 gm (Air frame of 6 gm, propulsion system of 36gm, and controls of 7 gm).
- Wingspan is set to a maximum of 15cm. This limitation is a standard target for an MAV.
- The wing shape is semicircular to make the maximum use of the area.
- The wing constant loading is obtained from equation (40) in W. Shyy, et al and assumes a cruising speed of 30-60Kph and a circular wing of diameter 15 cm:

$$\frac{W}{S} = \frac{mg}{S} = 27.8 N/m^2 \tag{6.1}$$

- The wing beat frequency is set to 10.4Hz.

6.2.2 Wing Designs

Due to its ability to model complex shapes of multilayer ionic transducers, the proposed FEA method was used to design two different MAV wings. The first wing was designed to be fully made of ionic polymer sheets.

It was designed as a semicircular wing to make the best use of the area covered (keeping the size of the MAV as small as possible) as shown in Figure 6.1. The radius was 7.5 cm, and it required 5 stacks of ionic polymer sheets (200m thick), to generate a displacement of 12 mm peak to peak tip displacement under the application of 28 N/m^2 lifts force at a frequency of 10.1 Hz. A second wing was developed and was composed of two different materials: the passive light material that forms the wing

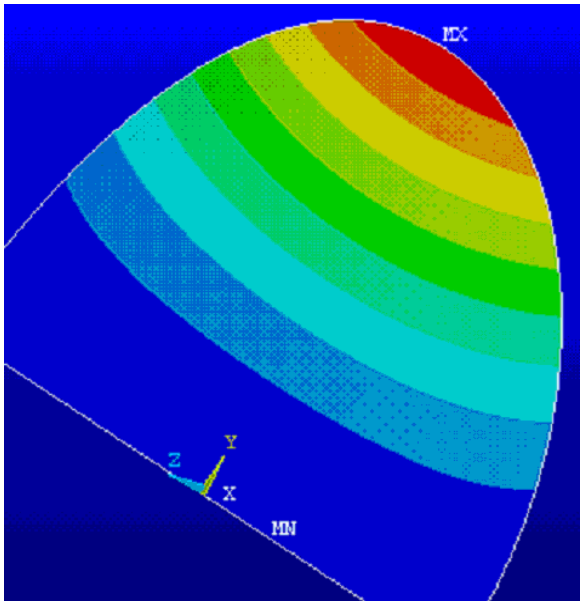

Figure 6.1: The deflection color map output of the FEA analysis of the first wing design.

surface, and a stack of 10 ionic polymer sheets of 7 x 5 cm size that performed as muscles to actuate the wing. The stack was able to deflect 8 mm at the tip under the application of 27.8N/m^2 force and frequency of 20.4Hz. Finally a 1.1 V actuation is safe enough to avoid electrolysis, which starts to occur at 1.22 volts. Thus in our design one can still increase the force by approximately 10%.

6.2.3 Comparison to requirements

The first wing design was close enough to the design requirements. The weight of the polymers was computed to be 41.4 gm. The polymer is to replace the propulsion system and the wings, therefore this will leave less than 10grms for the controls and the power source. This is considered to be a difficult constraint to meet, especially when considering the weight of the battery. As for the other loading conditions, they matched well the requirements. The second wing design has a polymer weight of 32.8gm of polymer. This is around 9gms less than the first design, but it is good to note that for this design a wing frame is required. As for the other parameters the tip peak to peak displacement is lower than the first design, but the beating frequency is much higher. These two results demonstrate that stacking the polymer

has the potential to produce a viable wing design, but these two designs have to be considered from the aerodynamics point of view before being considered acceptable. It is important to note that both designs could be made much more efficient if we able to consider a micro-layering process, in which we would be able to exert a higher potential per unit thickness without exceeding the electrolysis limit.

6.3 Summary

In this chapter two wing designs that operate as flapping MAV are presented. No aerodynamic computation was performed, rather we relied on data from Wei Shyy et al. (1999). The finite element analysis tool previously described in Chapter 3 was used to simulate the designs. The first wing was designed to be fully made of ionic transducer sheets. This wing is designed as 5 layers 200μm semicircular sheets connected in parallel. This design was able to meet all the requirements, but it's weight was computed to be 41.4 gm. The second design composed of ionic polymers as actuators, and a passive light material that forms the wing surface. Compared to the first design this wing is capable of less peak to peak deflection but operated at a higher frequency. The weight of the active material in this design was 32.8 gm. As a final conclusion ionic polymers were able to actuate the MAV, but they are heavy and left small load for the power storage or power generation and control devices.

Chapter 7

Summary and Conclusions

7.1 Introduction

In this chapter a brief summary of the whole thesis is provided. The contributions to the field are cited, and major conclusions are drawn. Finally in the last section some future work is proposed.

7.2 Thesis Summary

We have developed and characterized multilayer ionic transducers as series, parallel and combined stacks. In series stacking, ionic polymers are simply layered on top of each other. Parallel stacking is rather a more complicated way of wiring the polymers so they are electrically in parallel. On the other hand, parallel stacks significantly improved the performance regarding both actuation and sensing. As actuators, the electric potential per unit thickness was increased proportional to the number of layers in the parallel stack, resulting in larger transduction forces. Parallel stacking also enhanced the sensitivity, which is a function of the nature of the signal measuring circuit. The mechanical boundary condition represented in the polymer interfacial friction was also characterized. Increasing the interfacial friction increased the bandwidth while decreasing the free displacement of the polymer, and vice versa. A Finite Element Analysis (FEA) method was explained, verified, and used to numerically

validate the previous conclusions. It assumed an applied constant pressure load generated by each layer.

The combined stacks were presented and they consist of an actuation stack, layered on top of an insulated polymer and were used for feedback control in ionic polymers. The major problem in combined stacks was to eliminate the feed-through. Feedthrough is defined as the portion of the actuating signal of the adjacent ionic polymer that is directly fed through to the output signal of the sensor. The feed-through was mainly due the humidity in the gaps between stacks which created a short-circuit between the sensor and the actuator(s).

Newbury's equivalent circuit representation of ionic polymers was modified to accommodate the multilayer polymers. The modification was performed on four different boundary conditions, two electrical the series and the parallel connection, and two mechanical the zero interfacial friction and the zero slip on the interface. This modified model has the ability to model cantilever multilayer ionic transducers as sensors and actuators. It provides a transfer function that could be used in control, and system level design of ionic transducer devices.

By using the proposed FEA method and stacking technique we were able to design two different Micro Air Vehicle (MAV) wings. The first wing was designed to be fully made of ionic polymer sheets. It was designed as a semicircular wing to make the best use of the area covered (keeping the size of the MAV as small as possible). The second wing was developed and was composed of two different materials: the passive light material that forms the wing surface, and a stack of 10 ionic polymer sheets of 7 x 5 cm size that performed as muscles to actuate the wing. Finally the FEA numerical simulations indicated that ionic polymers have potentials to be considered for MAV applications, although the weight of the controls and power source would be a difficult constraint to meet in a practical application.

7.3 Contributions to the Field

The main contribution of this research is the development and characterization of a stacking process for ionic polymer materials. This multilayer stacking process was characterised for four different boundary conditions, and extended to the design of the combined multilayer transducers. The boundary conditions are the two electrical (series and parallel connections), and the two mechanical (no slip and no friction interfacial condition). Those boundary conditions provided the designer of polymer transducer base device the flexibility to increase the force output, the sensor sensitivity by using parallel connection. It also provided the ability to control the free displacement and structural resonance frequency by controlling the interfacial slip. If there is no slip the stack will behave as if it was one complete block, thus the natural frequencies will increase, while the large free displacement will be reduced. On the contrary if there is no friction between the faces, both the natural frequencies and the free displacement will be preserved. The combined stacks are designed to be used for feedback control in ionic polymers. They provided a compact device that incorporates a soft large deformation actuator, and a feedback sensor embedded inside the stack. Signal feed through proved to be the major difficulty in combined stacks. It could be reduced by increasing water insulation between the actuator and sensor stack.

Two modeling tools were presented, the finite element method and Newbury's empirical model. The FEA method is useful to model the peak force or displacement for complex actuator geometries. It could be used to model and analyze the interfacial friction boundary condition. Newbury's empirical model was modified to handle the multilayer transducers. This model is useful in determining both the sensing and the actuating transient responses of a simple cantilever ionic transducer beam. Both models were validated by successfully comparing them to experimental data.

Finally we proved that the multilayer ionic transducers could be used to design a flapping micro air vehicle.

7.4 Conclusion

Other than the tools and methods previously described two major conclusions can be made for the stacking technique. First it provided a control on the force and displacement output and sensitivty of the transducer. Connecting the layers in parallel reduces the voltage requirement of the mechanism and allows us to apply voltages that do not exceed the electrolysis limit. Also it provided an increase in bandwidth suitable for the desired operated frequencies. Next, electrical feed-through due to water transport is a key limitation when utilizing sensors and actuators for feedback control. This can be eliminated with proper packaging techniques and good layer-to-layer insulation.

7.5 Future work

The main target of this thesis was to enhance the performance of ionic polymers using stacking techniques. The hand layered parallel stacks helped increasing the generated force, but it also increased the weight or the amount of polymers used. On the other hand thinner layers in the parallel stack would help increasing the force without increasing the weight, resulting in higher energy capacity actuator. Thinner layers would also decrease the stiffness of the sensor layer in the combined stack, preserving the large free displacement of actuator stack in it. Therefore the efficiency of the multilayer techniques proposed in this thesis are well invested by decreasing the layer thickness.

Another problem we faced was the difficulty of fabricating parallel and combined stacks. Hand layering of a 3 layer parallel stack consumes around 2 hours, and the result might be a useless stack with short circuits in the connections. Therefore the automation of the layering process is a must.

A proposed future work is using Electronic Self Assembly (ESA) techniques in order to move the layering process to the micro level, and automate it. The ESA technique is composed of several steps, the major ones are the plasma treatment in

order to break the bonds on the surface, the next is to add a monolayer on this surface, than etching it using ultra violate light through a mask and finally deposit the gold on top of the monolayer. Furthermore ionic polymer solution such as Nafion™ could be used to build active polymer material, and an isolative polymer solution could be used for the insulation. ESA will contribute in etching a certain pattern on the surface enabling the layers to be connected in parallel for a parallel stack. This should also help in creating a more robust combined stack, by making the insulation between the two stacks more consistent.

Another improvement which would help reducing the feed through in the combined stack is the development of a current or charge sensor that doesn't require grounding either side of the sensor. This was briefly attempted during the research for this thesis without any success.

Furthermore, Newbury's model modification still requires further investigations. The extreme mechanical boundary conditions for the interfacial friction (no slip or no friction) are not general to cover all possibilities. The no friction boundary condition is virtually impossible. The stiffness of the insulation layer was also neglected in the model. Its effect might be large in some cases, especially in the combined stack where it is very critical to the feedthrough problem, and therefore we need a thick insulation. The last improvement in the model would be in accounting for the electric impedance across the insulation layer in the parallel stack, and the resistivity between the connections of the polymers in the series stack. The resistivity in the series stack is essentially small compared to resistivity of the ionic polymer, but it might become more pronounced in case the numbers of layers are increased, and their thickness decreased. As for the parallel stack, the capacitance introduced across the impedance is fairly large and might be comparable to the one across the ionic polymer.

Finally, new non-aqueous based ionic polymers are being developed within our group. Matt Bennett has successfully used ionic liquids as solvents for the new transducers. Ionic liquids have zero vapor pressure, and they also offer wider electrical stability. They are nonvolatile which reduces the need for packaging, and the wide

electrical stability provides larger operating voltages and therefore provides larger forces and displacement. The major limitation which is under current investigation is the slow response. We believe that thinner layers should be able to increase the response rate, since it will be a shorter travel to the ions across the transducer. Therfore micro-layered multalyer transducer might help in increasing the response rate of the ionic liquid based transducers. Furthermore the elimination of water would be a helpful for the feedthrough problem in the combined actuators.

Bibliography

Y. Bar-Cohen, Electroactive Polymer [EAP] Actuators as Artificial Muscles. Reality, Potential, and Challenges, SPIE Press, Chap 6 pp. 140–184, 2001.

Akle, B. and Leo, D., Multilayer Ionic Polymer Transducer, Submitted proceedings of the SPIE Smart Materials and Structures Conference, 2003.

Leo, D., ME5984: Smart Structures/ Active Material Systems, Virginia Tech courses, 2001.

Y. Bar-Cohen, S. Leary, M. Shahinpoor, J.O. Harrison, and J. Smith, Electro-Active Polymer (EAP) actuators for planetary applications, Proceeding of the SPIE, Vol. 3669, No. 1, pp. 57-62, 1999.

M. Shahinpoor, Y. Bar-Cohen, J.O. Simpson and J. Smith, Ionic Polymer-metal composites (IPMC) as biomimetic sensors and actuators, Proceeding of the SPIE's 5th Anual Symposioum on Smart Structures and Materials, Vol. 3324, No. 27, pp. 1-17, 1998.

K. M. Newbury, Characterization, Modeling, and Control of Ionic Polymer Transducers, PhD Dissertation, Virginia Tech, etd-09182002-081047, 2002.

Piezo Systems, Inc, URL: http://www.piezo.com/, Cambridge, Massashusetts.

W. Shyy, M. Berg and D. Ljungqvist, Flapping and Flexible Wings for Biological and Micro Air Vehicles, Progress in Aerospace Sciences, Vol. 35, No. 1, pp. 455-505, (1999).

K. M. Newbury, Leo, D. J., Electrically induced permanent strain in ionic polymer-metal composite actuators, Smart Structures and Materials Proc. SPIE Vol. 4695, pp. 67-77, 2002.

C. Kothera Micro-Manipulation and Bandwidth Characterization of Ionic Polymer Actuators, Master's Thesis, Virginia Tech, etd-12062002-110547, (2003).

M. Bennett and D. Leo, Ionic liquids as hyper-stable solvents for ionic polymer transducers, Submitted to the International Mechanical Engineering Congress and R&D Expo, (2003).

J. Shigley and C. Mischke, Mechanical engineering design, McGRAW-Hill International Editions Fifth edition, ME series, 1989.

Vita

I come from Zgharta, a town in north Lebanon where I lived until I moved to Beirut in 1996 to further my education at The American University of Beirut, where I graduated with distinction in 2001. I hold a B.S in Mechanical Engineering and in the summer of 2000 I did an internship at Universidad Carlos III de Madrid, where I designed an industrial Coriolis Effect Flow Meter to be used in hazardous liquids applications. In August of 2001, I moved to Virginia Tech to pursue my Masters Degree. I am currently working in the area of multilayer ionic transducers actuators with Dr. Don Leo at the Center for Intelligent Material Systems and Structures

Permanent Address: 300 Durham Hall
Blacksburg, VA 24061
United States of America

This thesis was typeset with LaTeX 2ε[1] by the author.

[1] LaTeX 2ε is an extension of LaTeX. LaTeX is a collection of macros for TeX. TeX is a trademark of the American Mathematical Society. The macros used in formatting this thesis were written by Greg Walker, Department of Mechanical Engineering, Virginia Tech.